ORIGINAL RESEARCH

MTOR suppresses autophagy-mediated production of IL25 in allergic airway inflammation

Wen Li,[1] Yinfang Wu,[1] Yun Zhao,[1] Zhouyang Li ,[1] Haixia Chen,[1] Lingling Dong,[1] Huiwen Liu,[1] Min Zhang,[1] Yanping Wu,[1] Jiesen Zhou,[1] Juan Xiong,[1] Yue Hu,[1] Wen Hua,[1] Bin Zhang,[1] Minzhi Qiu,[2] Qing-ling Zhang,[2] Chunhua Wei,[3] Mingchun Wen,[3] Jing Han,[3] Xiaobo Zhou,[4] Weiliang Qiu,[4] Fugui Yan,[1] Huaqiong Huang,[1] Songmin Ying,[1] Augustine M K Choi,[5] Huahao Shen,[1,2] Zhihua Chen[1]

► Additional material is published online only. To view please visit the journal online (http://dx.doi.org/10.1136/thoraxjnl-2019-213771).

For numbered affiliations see end of article.

Correspondence to
Zhihua Chen; zhihuachen@zju.edu.cn
Huahao Shen; huahaoshen@zju.edu.cn

WL, YW and YZ contributed equally.

Received 27 June 2019
Revised 27 July 2020
Accepted 29 July 2020
Published Online First 15 October 2020

Check for updates

© Author(s) (or their employer(s)) 2020. No commercial re-use. See rights and permissions. Published by BMJ.

To cite: Li W, Wu Y, Zhao Y, *et al*. *Thorax* 2020;**75**:1047–1057.

ABSTRACT

Introduction Airway epithelial cells are recognised as an essential controller for the initiation and perpetuation of asthmatic inflammation, yet the detailed mechanisms remain largely unknown. This study aims to investigate the roles and mechanisms of the mechanistic target of rapamycin (MTOR)–autophagy axis in airway epithelial injury in asthma.

Methods We examined the MTOR–autophagy signalling in airway epithelium from asthmatic patients or allergic mice induced by ovalbumin or house dust mites, or in human bronchial epithelial (HBE) cells. Furthermore, mice with specific MTOR knockdown in airway epithelium and autophagy-related *lc3b*$^{-/-}$ mice were used for allergic models.

Results MTOR activity was decreased, while autophagy was elevated, in airway epithelium from asthmatic patients or allergic mice, or in HBE cells treated with IL33 or IL13. These changes were associated with upstream tuberous sclerosis protein 2 signalling. Specific MTOR knockdown in mouse bronchial epithelium augmented, while LC3B deletion diminished allergen-induced airway inflammation and mucus hyperproduction. The worsened inflammation caused by MTOR deficiency was also ameliorated in *lc3b*$^{-/-}$ mice. Mechanistically, autophagy was induced later than the emergence of allergen-initiated inflammation, particularly IL33 expression. MTOR deficiency increased, while knocking out of LC3B abolished the production of IL25 and the eventual airway inflammation on allergen challenge. Blocking IL25 markedly attenuated the exacerbated airway inflammation in MTOR-deficiency mice.

Conclusion Collectively, these results demonstrate that allergen-initiated inflammation suppresses MTOR and induces autophagy in airway epithelial cells, which results in the production of certain proallergic cytokines such as IL25, further promoting the type 2 response and eventually perpetuating airway inflammation in asthma.

Key messages

What is the key question?

► What is the main function of the mechanistic target of rapamycin (MTOR)–autophagy pathway in airway epithelial cells in allergic airway inflammation?

What is the bottom line?

► Decreased MTOR and/or enhanced autophagy in airway epithelial cells results in the production of proallergic cytokines, further promoting the type 2 response and the overall allergic airway inflammation.

Why read on?

► This is the first study to investigate the functions of MTOR–autophagy in airway epithelial cells in asthma pathogenesis.

INTRODUCTION

Asthma is characterised by allergic airway inflammation, mucus hyperproduction and remodelling, which eventually lead to bronchial hyperreactivity and airway obstruction.[1–3] The airway epithelial cells (ECs) are recognised as an essential controller for the initiation and perpetuation of asthmatic inflammation.[2 3] In response to allergens, ECs secrete endogenous danger signals such as thymic stromal lymphopoietin (TSLP) and granulocyte-macrophage colony-stimulating factor, thereby activating dendritic cells and bridging the innate and adaptive immunity. The initially recruited T cells and eosinophils secrete cytokines and chemokines and cooperatively cause further injury of ECs,[2 3] which in turn produce various proinflammatory mediators, such as IL25, IL33 and eotaxins, to amplify and perpetuate the allergic inflammation.[2 3] Thus, the injury of ECs contributes significantly to asthma pathogenesis; however, the detailed injury mechanisms of ECs in asthma remain largely unknown.

Mechanistic target of rapamycin (MTOR) kinase and its key downstream process autophagy play crucial roles in major cellular processes such as metabolism and proliferation.[4 5] MTOR is a serine/threonine protein kinase belonging to the PI3K-related kinase family. It interacts with several other molecules to form two distinct complexes named MTOR complex 1 (MTORC1) and MTORC2, which play distinct roles in pathophysiology.[4]

Thorax: first published as 10.1136/thoraxjnl-2019-213771 on 18 October 2020. Downloaded from http://thorax.bmj.com/ on December 26, 2020 at University of Liverpool Library. Protected by copyright.

Autophagy is a dynamic process responsible for the lysosomal degradation of damaged protein, damaged organelles and microorganisms, whose process includes initiation, elongation and formation of autophagosome (AP), and AP–lysosome fusion.[5] In general, MTORC1 is known as a major negative regulator of autophagy. MTORC1 may interact with and phosphorylate the Unc-51-like kinase 1, thereby suppressing autophagy.[5]

Recently, we and others have demonstrated that autophagy, in some cases together with MTOR, plays pivotal roles in numerous pulmonary diseases, including COPD, acute lung injury, pulmonary fibrosis and asthma.[6] A previous study has demonstrated a genetic association of autophagy related with asthma and has shown increased autophagic vacuoles (AVs) in ECs and fibroblasts from human asthmatics.[7] IL13 could activate autophagy, while impairment of autophagy results in decreased MUC5AC secretion and subsequently increases MUC5AC staining in human airway ECs.[8] CD11c-specific *atg5*$^{-/-}$ mice displayed an IL17A-dependent neutrophilic inflammation induced by house dust mites (HDM).[9] Altogether, these data suggest that the functions of autophagy in asthma pathogenesis are likely cell specific. Moreover, several studies have indicated that inhibition of MTOR using rapamycin attenuates allergic airway inflammation,[10–13] suggesting a protective role of MTOR inhibition in asthma. However, pulmonary toxicity has been widely observed when rapamycin is used as an immunosuppressive drug for renal transplantation.[14] Thus, the roles of MTOR in asthma should also be cell type-dependent. Nevertheless, little is known about the functions of MTOR and autophagy in ECs in asthma pathogenesis.

The present study aims to explore the functions of MTOR and autophagy in ECs in allergic inflammation, by examining the MTOR–autophagy signalling in bronchial specimens from human asthmatics, and the dysregulated airway inflammation in MTOR-impaired or autophagy-impaired mice. We also provide evidence that the functions of MTOR–autophagy signalling in ECs in allergic inflammation mechanistically link to the production of proallergic cytokines.

METHODS

Detailed descriptions of methods are provided in the online supplementary.

Human samples

The patients' clinical data are described in tables 1 and 2. More detailed information can be found in the online supplementary.

Table 1 Characteristics of human subjects for p-S6 and LC3B expression

	Healthy controls	Asthma	P value
Number	3	12	–
Age, years	49 (43–67)	53 (42–59.75)	0.822
Sex (M/F)	2/1	6/6	–
Bronchodilator reversibility test	Negative	Positive	–
Blood eosinophils (%)	0 (0–1.2)	4.75 (3.075–16.3)	0.004
FEV_1, % predicted	105.9 (90–112)	62.6 (49.35–76.38)	0.009

Data are presented as median±IQR. Differences between groups were assessed by Mann-Whitney U test where p<0.05 is significant.
FEV_1, forced expiratory volume in one second; M/F, male/female.

Table 2 Characteristics of human subjects for TEM experiment

	Healthy controls	Asthma	P value
Number	4	4	–
Age, years	55 (49.5–59.75)	55.5 (53.5–59)	0.971
Sex (M/F)	2/2	2/2	–
Bronchodilator reversibility test	Negative	Positive	–
Blood eosinophils (%)	2.4 (1.575–3.75)	7 (3.425–9.525)	0.114
Blood eosinophils, $\times 10^9$/L	0.095 (0.038–0.145)	0.535 (0.23–0.675)	0.057
FEV_1, % predicted	89.5 (84.41–94.5)	64.35 (54.23–73.58)	0.029

Data are presented as median±IQR. Differences between groups were assessed by Mann-Whitney U test where p<0.05 is significant.
FEV_1, forced expiratory volume in one second; TEM, transmission electron microscopy .

Mice

mtor$^{flox/flox}$ mice (C57BL/6; The Jackson Laboratory; Bar Harbor, USA) were crossed with CC10-rtTA/(tetO)^7-cre transgenic mice (C57BL/6) to generate CC10-rtTA/(tetO)^7-cre-*mtor*$^{flox/flox}$ (*mtor*$^{\Delta/\Delta}$) mice. *lc3b*$^{-/-}$ mice were from Jackson laboratory. More detailed information of animal experiments is shown in the online supplementary. All experimental protocols were in line with the Animal Research Reporting of In vivo Experiments (ARRIVE) guidelines.[15] A completed ARRIVE guideline checklist was included in checklist S1.

Statistics

Statistical tests were analysed using GraphPad Prism software (V.7.0; San Diego, CA, USA). The normality of data was analysed using Kolmogorov-Smirnov test. Normally distributed data were assessed by using a parametric statistical test (t-test for differences between two groups, one-analysis of variance for those between multiple groups) and were presented as mean±SEM. While non-normally distributed data were analysed using a non-parametric statistical test (Mann-Whitney U test for differences between two groups, Kruskal-Wallis H test for those between multiple groups) and presented as median±IQR. Differences were considered significant when $p<0.05$.

RESULTS

Dysregulation of MTOR–autophagy in ECs from asthmatic patients or experimental allergic mice

We first explored the MTOR–autophagy signalling in bronchial specimens of asthmatic patients. Interestingly, the MTOR activity, as revealed by the immunohistochemical staining of p-S6 (phosphorylated ribosomal protein S6),[4] was significantly decreased, while autophagy-related hallmark LC3B (microtubule-associated protein 1 light chain 3)[16] was markedly elevated (figure 1A and B) in ECs from asthmatics relative to healthy controls. Consistently, AVs were also apparently evident in ECs from asthmatic patients (figure 1C and D). Immunostaining revealed a markedly decreased p-S6 in airway ECs of allergic mice induced by HDM extract (figure 1E and F). After the last challenge of HDM, the airway epithelium appeared as normal with very few AVs observed at 24 hours (figure 1G and H). However, the number of APs was significantly increased at 48 hours, and autolysosomes (ALs) emerged later at 72 hours post-HDM exposure (figure 1G and H), suggesting a time-dependent induction of autophagy in ECs during allergic inflammation.

Thorax: first published as 10.1136/thoraxjnl-2019-213771 on 18 October 2020. Downloaded from http://thorax.bmj.com/ on December 26, 2020 at University of Liverpool Library. Protected by copyright.

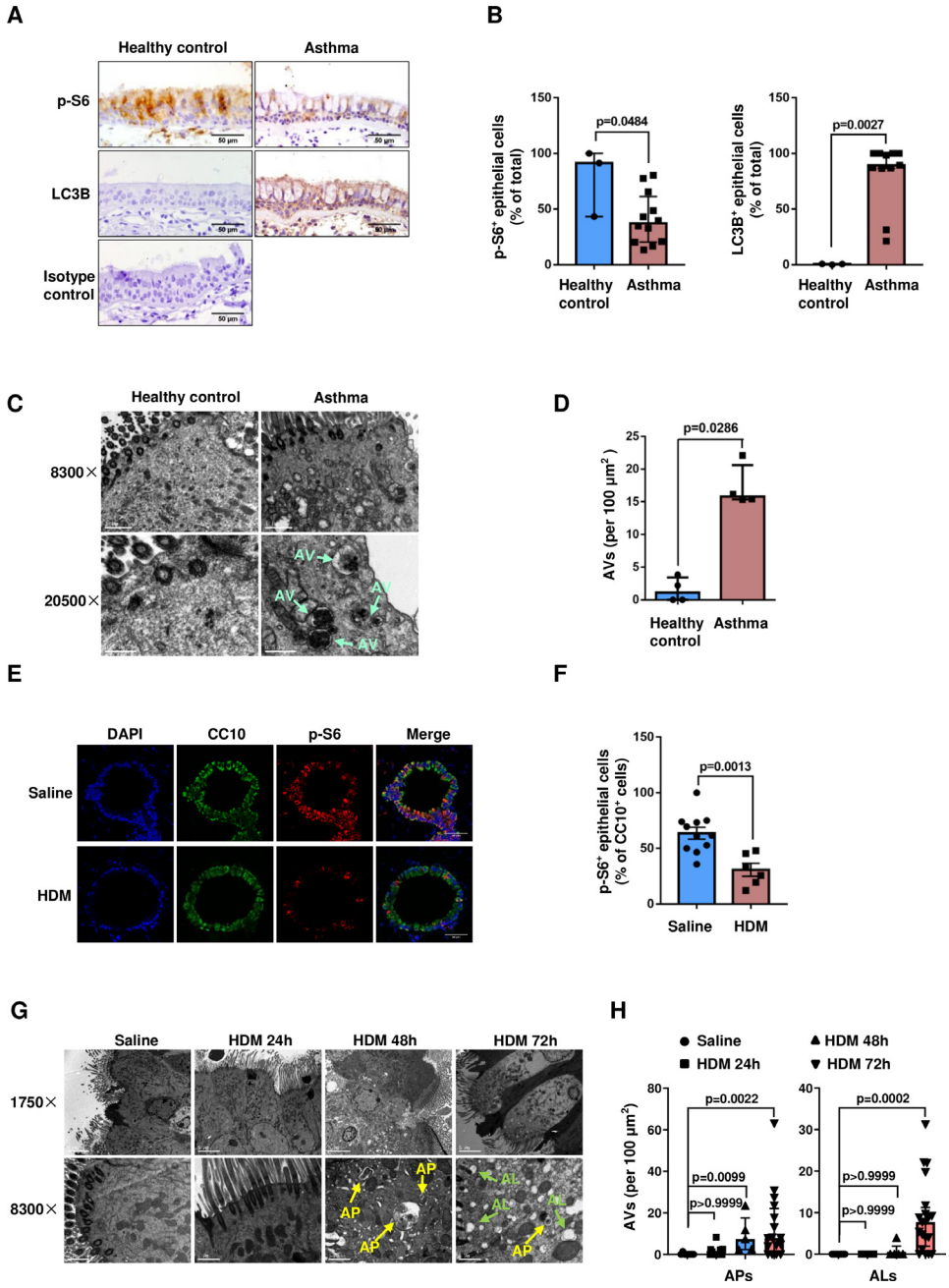

Figure 1 Dysregulated MTOR–autophagy in the airway epithelium of asthmatic patients or allergic mice. (A and C) Representative images of immunohistochemistry staining of p-S6 (A, upper panels) or LC3B (A, lower panels) (scale bar: 50 μm), or electronic microscopy (EM) analysis of AVs (C) (scale bar: 8300×, 1 μm, 20 500×, 0.5 μm) in bronchial specimens from healthy controls or asthmatic patients. (B and D) Semiquantification of the expression of p-S6 (B, left panels), LC3B (B, right panels) or AVs (D) in the bronchial specimens. Data (A and B) are representative of three healthy controls and 11–12 asthmatic patients, whose clinical information is shown in table 1. Data (C and D) are representative of four healthy controls and four asthmatic patients, whose information is shown in table 2. (E and F) Representative images (E) and semiquantified results (F) of the costaining of CC10 and p-S6 in mouse lung sections 72 hours after HDM challenge. Scale bar: 50 μm. Randomly selected two to three areas of each sample were used for semiquantification. (G and H) Representative images (G) and semiquantified results (H) of the AVs in mouse airway epithelium after HDM challenge. Scale bar: 1750×, 5 μm, 8300×, 1 μm. Randomly selected two to four areas of each sample were used for semiquantification. Data (E–H) are representative of three independent experiments (three to six mice for each group). Error bars, mean±SEM (F) or median±IQR (B, D and H). AL, autolysosome; AP, autophagosome; AV, autophagic vacuole; HDM, house dust mite; MTOR, mechanistic target of rapamycin

Time course analysis of airway inflammation and allergic cytokines post-HDM challenge

To further understand how autophagy is regulated in allergic inflammation in vivo, we performed a time course analysis of inflammatory cells, IL13, IL25 and IL33 post-HDM challenge. Interestingly, neutrophils were dramatically increased at 24 hours and were declined to basal levels at 72 hours (figure 2A), while eosinophils and allergic cytokines such as IL13 and IL25 were increased unremittingly (figure 2A–2E). The levels of IL33, however, were peaked earlier at 24 hours and was decreased thereafter, but kept higher in allergic mice than those in control mice at 72 hours (figure 2F and G),

Thorax: first published as 10.1136/thoraxjnl-2019-213771 on 18 October 2020. Downloaded from http://thorax.bmj.com/ on December 26, 2020 at University of Liverpool Library. Protected by copyright.

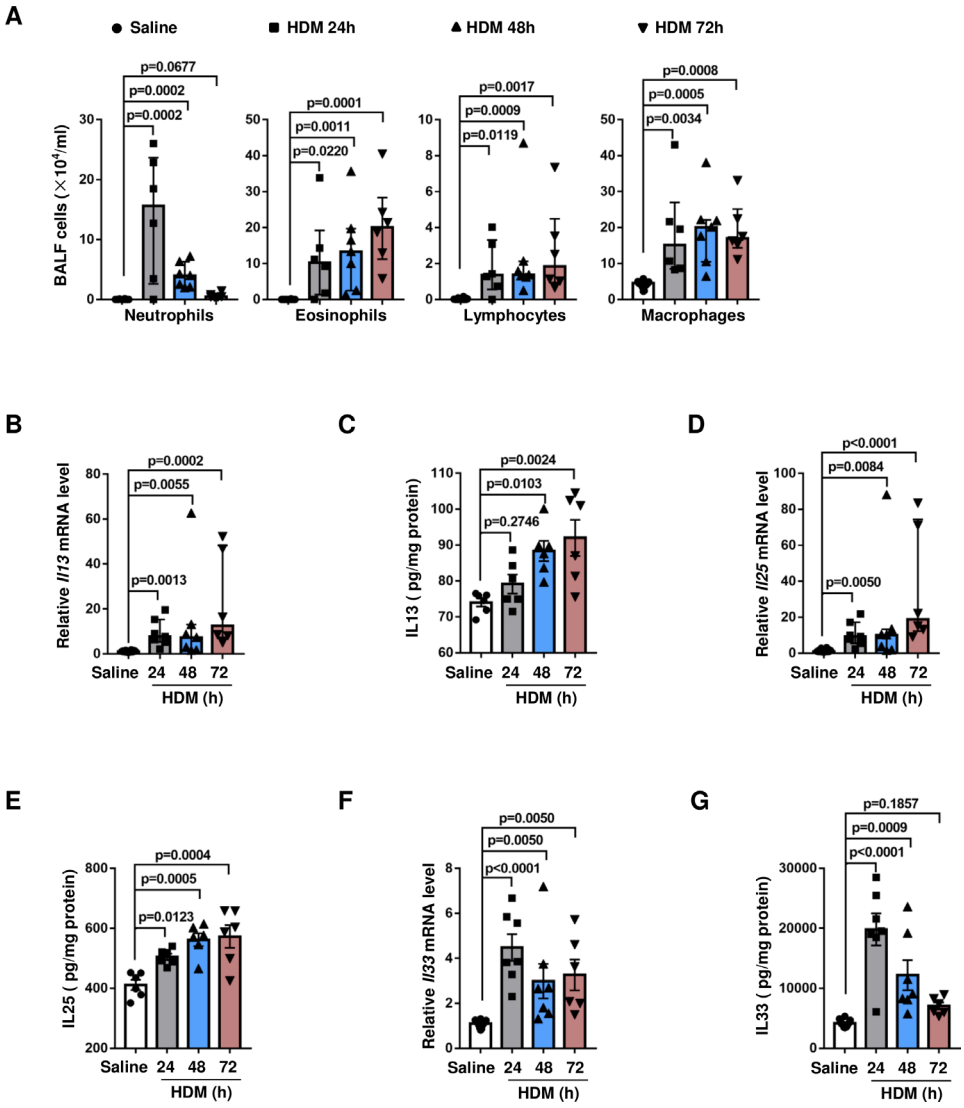

Figure 2 Time course of HDM-induced airway inflammation in mice. Mice were sacrificed at 24, 48 or 72 hours after the last HDM challenge. (A) Amounts of various inflammatory cells in BALF. (B–G) Expression of the inflammatory cytokines in lung homogenates. (B) *Il13* mRNA; (C) IL13 protein; (D) *Il25* mRNA; (E) IL25 protein; (F) *Il33* mRNA and (G) IL33 protein. Data (A–G) are representative of 6–14 mice for each group and were replicated in three independent experiments. Error bars, median±IQR (A, B and D) or mean±SEM (C, E, F and G). BALF, bronchoalveolar lavage fluid; HDM, house dust mite.

suggesting that the quick induction of IL33 may serve as a master switch to initiate the allergic inflammation. Together with the data that autophagy was only elevated after 48 hours (figure 1G and H), these findings suggested that the levels of MTOR and autophagy in ECs were most likely regulated by the early initiated inflammatory factors such as IL33.

Allergic cytokines IL33 and IL13 suppress MTOR and induce autophagy in HBE cells

Next, we sought to confirm the role of allergic cytokines in the modulation of MTOR–autophagy in cultured human bronchial epithelial (HBE) cells. IL33 is known as an early driver of allergic inflammation,[17] and it was induced quite early in our animal models (figure 2F and G). HBE cells also expressed relatively high levels of IL33 receptor ST2 (data not shown). Also, IL13 has been shown to induce autophagy in primary human tracheal ECs.[8] Therefore, we treated HBE cells with IL33 or IL13. Both cytokines exerted no effects on the cell viability at the current treatment conditions (data not shown). Consistently, IL33 or IL13 treatment significantly induced GFP-LC3 punctate in HBE cells (figure 3A and E). Both cytokines time-dependently decreased the levels of p-MTOR, while increased the expression of LC3B-II (figure 3B, C, F and G). Treatment of IL33 or IL13 with a lysosome inhibitor bafilomycin A_1 (Baf A1) further enhanced the induction of LC3B-II (figure 3D and H, online supplementary figure S1A and S1B), suggesting that the increased levels of LC3B-II by IL13 or IL33 treatment were indeed induced, rather than due to an impaired AP–lysosome fusion. Additionally, we examined the effects of some other cytokines on inducing autophagy in HBE cells. Interestingly, we found that another allergic cytokine IL4 failed to induce any appreciable changes on p-MTOR and LC3B-II (online supplementary figure S2A), while TNF-α even slightly suppressed LC3B-II (online supplementary figure S2B). These data suggested that not all proinflammatory cytokines could induce autophagy in HBE cells.

Thorax: first published as 10.1136/thoraxjnl-2019-213771 on 18 October 2020. Downloaded from http://thorax.bmj.com/ on December 26, 2020 at University of Liverpool Library. Protected by copyright.

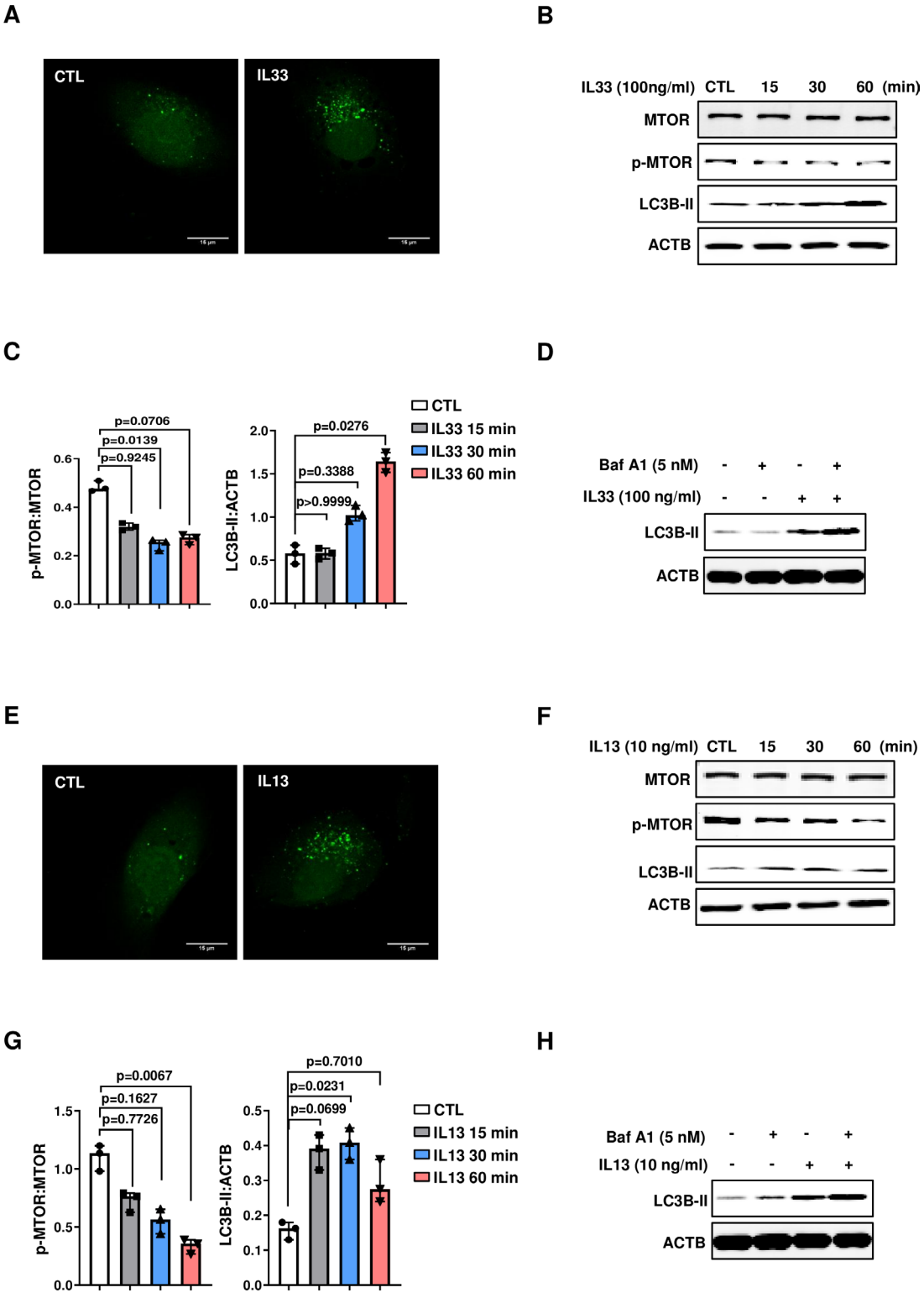

Figure 3 Allergic cytokines IL33 and IL13 suppress MTOR and induce autophagy in HBE cells. (A and E) Representative images of the punctate staining of GFP–LC3B in HBE cells treated with or without 100 ng/mL IL33 (A) or 10 ng/mL IL13 (E) for 0.5 hour. Scale bar: 15 µm. (B, C, F and G) Immunoblotting analysis of MTOR–autophagy-related molecules in HBE cells treated with IL33 (B and C) or IL13 (F and G) for indicated time points. (D and H) Levels of LC3B in HBE cells after IL33 (D) or IL13 (H) stimulation with or without Baf A1 (5 nM) at 0.5 hour. Data are representative of three independent experiments, and blots were quantified by ImageJ software. Error bars, median±IQR. HBE, human bronchial epithelial; MTOR, mechanistic target of rapamycin

Dysregulated TSC2 in ECs in allergic inflammation

We next sought to determine the upstream signalling which modulates MTOR–autophagy in ECs during allergic airway inflammation. TSC1/2 (TSC, tuberous sclerosis protein) is known as a central regulator of MTOR. Consistent with the decreased levels of MTOR and increased autophagy, the expression of p-TSC2 was significantly

Thorax: first published as 10.1136/thoraxjnl-2019-213771 on 18 October 2020. Downloaded from http://thorax.bmj.com/ on December 26, 2020 at University of Liverpool Library. Protected by copyright.

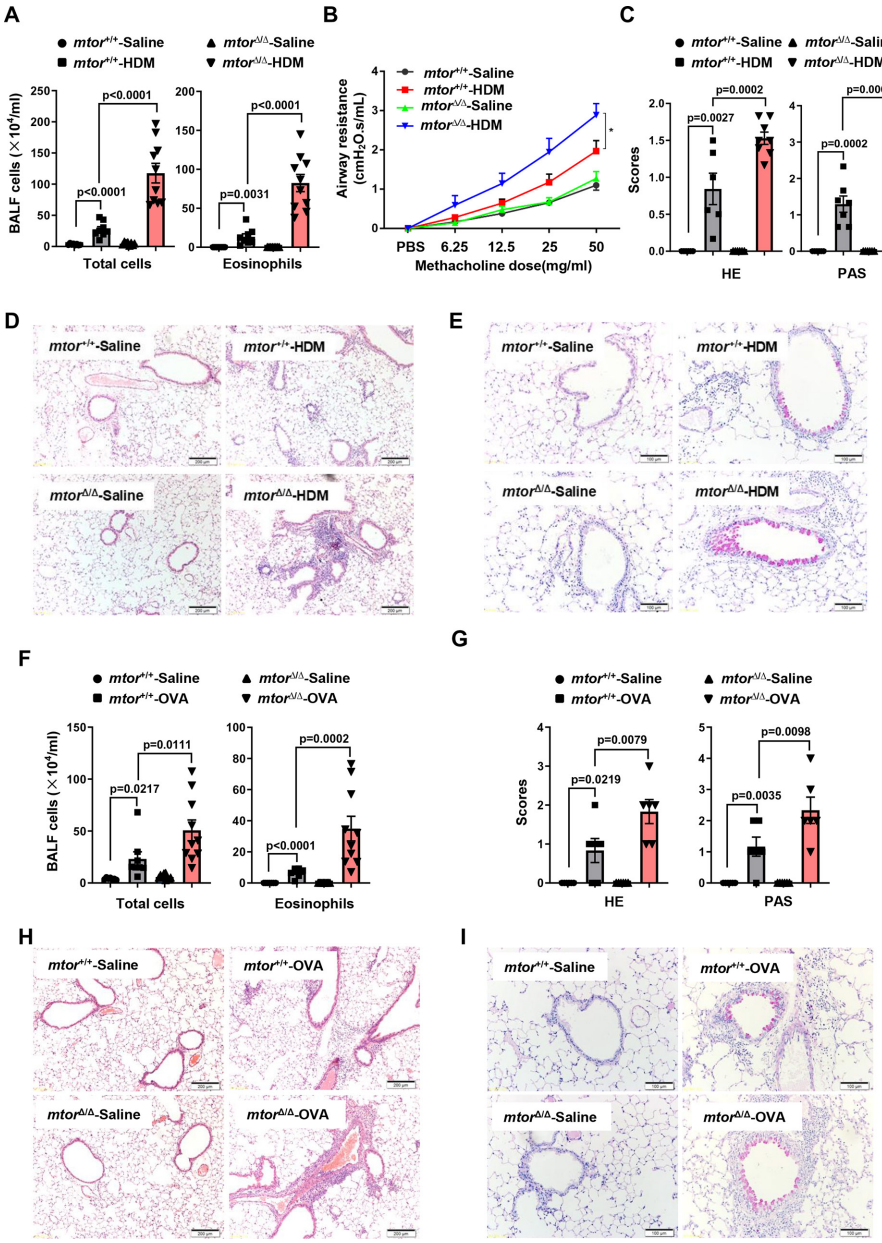

Figure 4 Specific knockdown of MTOR in mouse bronchial epithelial cells exacerbates allergen-induced airway injury and inflammation. *mtor*$^{\Delta/\Delta}$ mice were sacrificed 72 hours after the last HDM challenge or 24 hours after the last OVA challenge. (A and F) Amounts of total inflammatory cells and eosinophils in BALF induced by HDM (A) or OVA (F) challenge. (B) AHR in response to methacholine in *mtor*$^{\Delta/\Delta}$ mice was measured 48 hours after the last exposure to HDM. (C and G) Semiquantified score of the H&E or PAS staining in mouse lungs challenged with HDM (C) or OVA (G). (D and H) Representative images of H&E staining in mouse lungs with HDM (D) or OVA (H) challenge. Scale bar: 200 µm. (E and I) Representative images of PAS staining in mouse lungs with HDM (E) or OVA (I) challenge. Scale bar: 100 µm. Data are representative of 6–10 mice for each group and were replicated in three independent experiments. Error bars, mean±SEM. BALF, bronchoalveolar lavage fluid; HDM, house dust mite; OVA, ovalbumin; PAS, periodic acid-Schif.

increased in ECs from asthmatic patients (online supplementary figure S3A and S3B) or allergic mice (online supplementary figure S3C and S3D). The net amount of TSC2 and its phosphorylation were significantly induced in IL13-treated HBE cells (online supplementary figure S3E and S3F), while the p-TSC2:TSC2 ratio remained unchanged (online supplementary figure S3G). All these data suggested that the dysregulation of the MTOR–autophagy pathway might be associated with TSC2 signalling in ECs in allergic inflammation.

EC-localised MTOR suppresses airway injury and allergic inflammation in mice

To examine the functions of airway-specific MTOR in allergic airway inflammation, mice with specific knockdown of *mtor* in airway epithelium (*mtor*$^{\Delta/\Delta}$) (online supplementary figure S4A-S4C) were used. We utilised two well-accepted allergic mouse models using HDM or ovalbumin, respectively. Intriguingly, in both models, the *mtor*$^{\Delta/\Delta}$ mice exhibited a significantly augmented allergic inflammation, as evidenced by the further increased inflammatory cells and eosinophils in bronchoalveolar lavage fluid (BALF) (figure 4A and F), the largely exacerbated inflammation around airways (figure 4C, D, G and H) and the highly enhanced mucus accumulation (figure 4C, E, G and I). The expression of allergy-related cytokines and mucin, such as *Il13*, *Il33* and *Mu5ac* (mucin 5AC, oligomeric mucus/gel forming), was also further induced in *mtor*$^{\Delta/\Delta}$ mice (online supplementary

Thorax: first published as 10.1136/thoraxjnl-2019-213771 on 18 October 2020. Downloaded from http://thorax.bmj.com/ on December 26, 2020 at University of Liverpool Library. Protected by copyright.

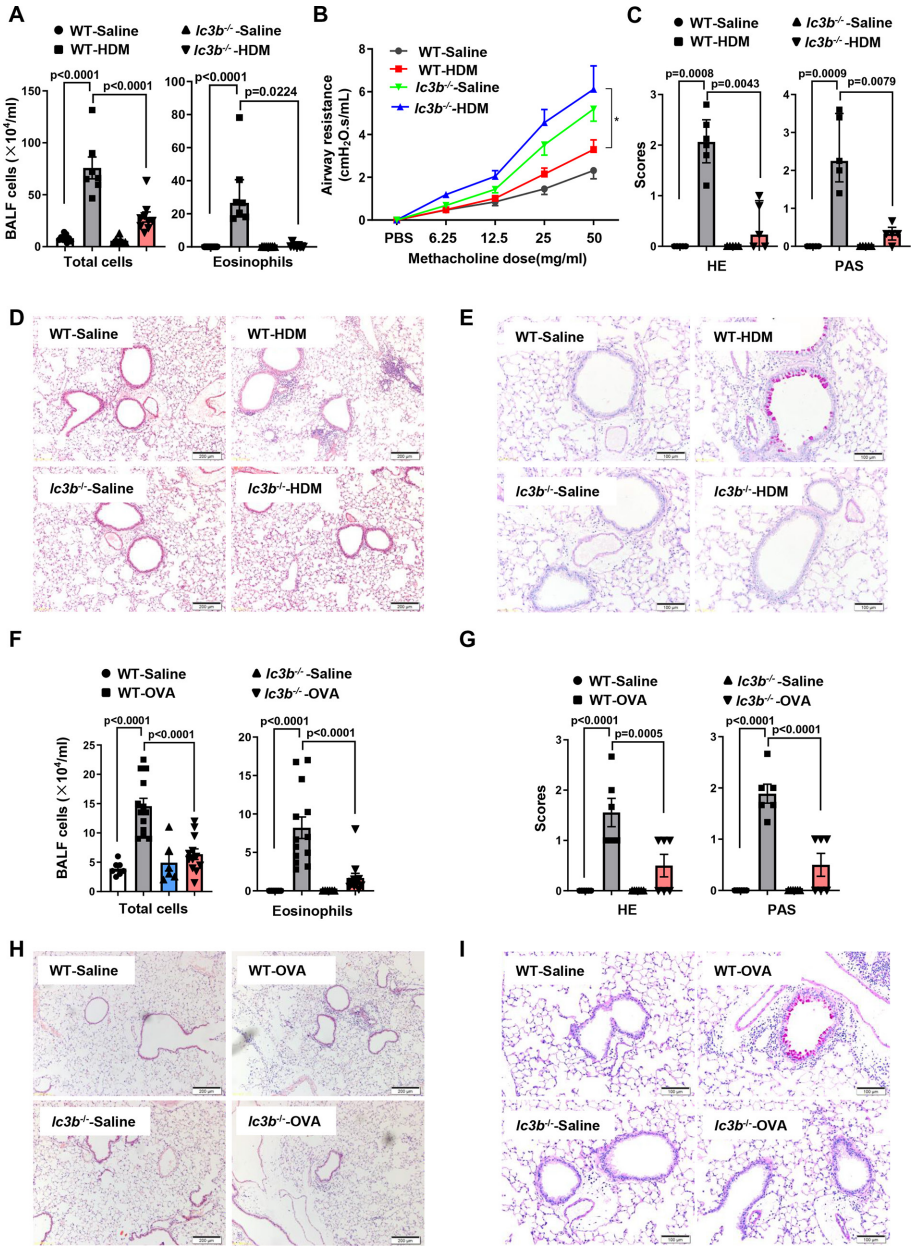

Figure 5 Knockout of *LC3B* abolishes allergen-induced airway injury and inflammation.*lc3b*$^{-/-}$ mice were sacrificed 72 hours after the last HDM challenge or 24 hours after the last OVA challenge. (A and F) Amounts of total inflammatory cells and eosinophils in BALF induced by HDM (A) or OVA (F) challenge. (B) AHR in response to methacholine in lc3b-/- mice was measured 48 hours after the last exposure to HDM. (C and G) Semiquantified score of the H&E or PAS staining in mouse lungs challenged with HDM (C) or OVA (G). (D and H) Representative images of H&E staining in mouse lungs with HDM (D) or OVA (H) challenge. Scale bar: 200 µm. (E and I) Representative images of PAS staining in mouse lungs with HDM (E) or OVA (I) challenge. Scale bar: 100 µm. Data are representative of 5–13 mice for each group and were replicated in three independent experiments. Error bars, median±IQR (A, right panels, and D) or mean±SEM (A, left panels, E, and H). BALF, bronchoalveolar lavage fluid; HDM, house dust mite; OVA, ovalbumin.

figure S5A-S5C). The *mtor*$^{\triangle/\triangle}$ mice also exhibited further increased airway hyperresponsiveness (AHR)relative to the controls in response to HDM treatment (figure 4B).

Knockout of LC3B abolishes allergen-induced airway injury and inflammation in mice

To investigate the role of autophagy in allergic inflammation, *lc3b*$^{-/-}$ mice which demonstrate impaired autophagy in lungs and other organs[18 19] were used. In contrast to the results of *mtor* deficiency, *lc3b*$^{-/-}$ mice displayed an almost completely abolished phenotype in both allergic models, with markedly reduced allergic inflammation in BALF (figure 5A and F) and around airways (figure 5C, D, G and H), and diminished mucus production (figure 5C, E, G and I). Consistent with these, the mRNA levels of Il13, Il33, Muc5ac, Il5 and Eotaxin 1 induced by allergens were also dramatically attenuated in *lc3b*$^{-/-}$ mice (online supplementary figure S5D-S5H). However, the *lc3b*$^{-/-}$ mice surprisingly displayed a significantly increased AHR compared with wild-type (WT) littermates on HDM exposure (figure 5B), which was completely opposite to the results of airway inflammation.

To further confirm the function of autophagy in allergic airway inflammation, mice were treated with spautin-1, a specific autophagy inhibitor[20] which has been shown to attenuate the particulate-induced airway inflammation.[21]

Thorax: first published as 10.1136/thoraxjnl-2019-213771 on 18 October 2020. Downloaded from http://thorax.bmj.com/ on December 26, 2020 at University of Liverpool Library. Protected by copyright.

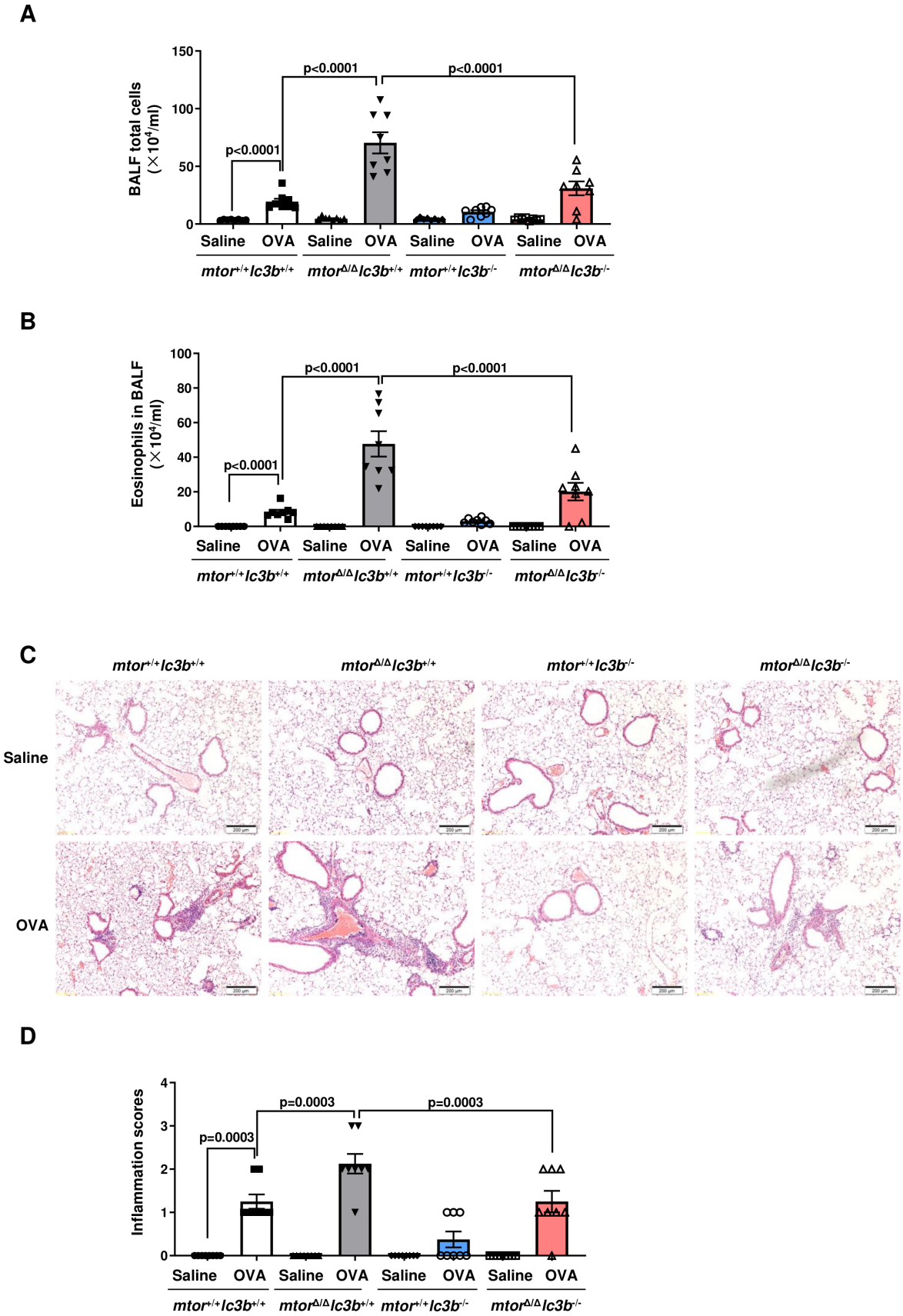

Figure 6 Knockout of *LC3B* ameliorates the exacerbated inflammation caused by MTOR deficiency. (A and B) Amounts of total inflammatory cells (A) and eosinophils (B) in BALF induced by OVA challenge. (C and D) Representative images (C) and semiquantified score (D) of H&E staining in mouse lungs with OVA challenge. Scale bar: 200 µm. Data are representative of eight mice for each group and were replicated in three independent experiments. Error bars, mean±SEM. BALF, bronchoalveolar lavage fluid; HBE, human bronchial epithelial; HDM, house dust mite; MTOR, mechanistic target of rapamycin; OVA, ovalbumin.

Thorax: first published as 10.1136/thoraxjnl-2019-213771 on 18 October 2020. Downloaded from http://thorax.bmj.com/ on December 26, 2020 at University of Liverpool Library. Protected by copyright.

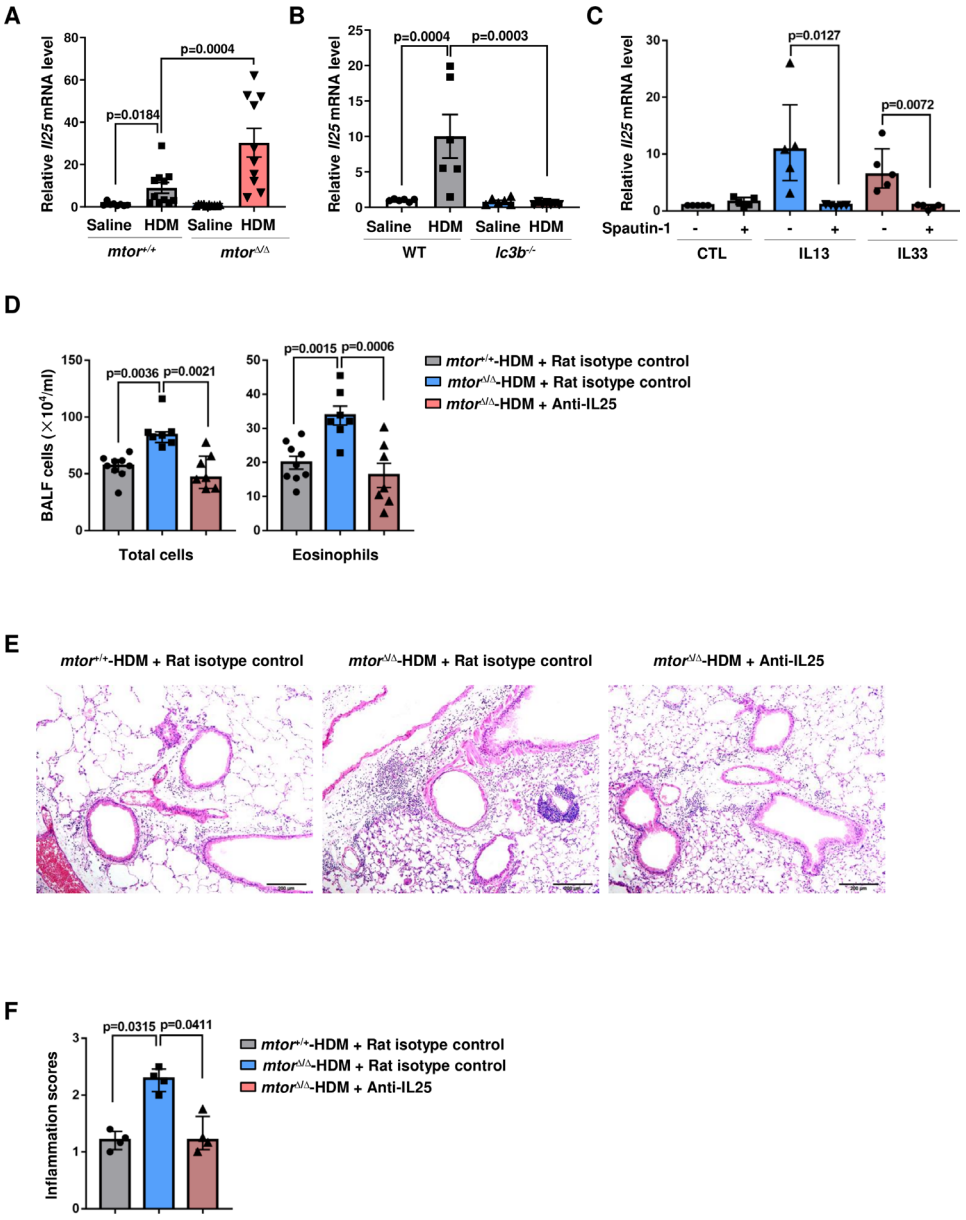

Figure 7 The MTOR–LC3B axis orchestrates the production of proallergic cytokines to promote the overall airway inflammation in allergic mice. (A and B) The mRNA levels of *Il25* in lung tissues of *mtor*$^{\Delta/\Delta}$ (A) or *lc3b*$^{-/-}$ (B) mice with HDM challenge. Mice were sacrificed 72 hours after the last HDM challenge. (C) Effects of spautin-1 (10 nM) on the expression of *Il25* mRNA induced by IL13 or IL33. HBE cells were treated as indicated for 3 hours and were harvested for quantitative PCR analysis. (D) Amounts of total inflammatory cells and eosinophils in BALF in *mtor*$^{\Delta/\Delta}$ mice treated with IL25 neutralisation antibody. (E and F) Representative images (E) and semiquantified score (F) of H&E staining in mouse lungs with OVA challenge. Scale bar: 200 µm. Data are representative of 4–11 mice for each group. All data were replicated in three independent experiments. Error bars, median±IQR (C, D left panels), (F) or mean±SEM (A, B and D right panels). BALF, bronchoalveolar lavage fluid; HBE, human bronchial epithelial; HDM, house dust mite; MTOR, mechanistic target of rapamycin; OVA, ovalbumin.

Interestingly, spautin-1 remarkably decreased HDM-induced eosinophilic inflammation and the expression of allergic cytokines (online supplementary figure S6A-S6E). Furthermore, spautin-1 significantly increased the AHR of allergic mice, in complete agreement with the results of *lc3b*$^{-/-}$ mice (online supplementary figure S6F).

LC3B in non-myeloid cells is essential for allergen-induced airway inflammation

The role of autophagy in disease pathogenesis is generally cell type-dependent.[6] To further confirm the role of non-myeloid LC3B in allergic inflammation, WT or *lc3b*$^{-/-}$ mice were reconstituted with WT or *lc3b*$^{-/-}$ bone marrow (online supplementary figure S7A and S7B). Interestingly, the *lc3b*$^{-/-}$ mice transferred with WT bone marrow showed a similar protective effect on the airway inflammation (online supplementary figure S7C-S7E). However, WT mice receiving *lc3b*$^{-/-}$ bone marrow also displayed a decreased airway inflammation (online supplementary figure S7C-S7E). These data altogether suggest that LC3B, either in certain myeloid or non-myeloid cells, is essential for orchestrating the overall allergic inflammation.

Knockout of LC3B ameliorates the exacerbated inflammation caused by MTOR deficiency

MTOR regulates a plethora of biological processes.[4] To determine whether the function of EC-localised MTOR in

Thorax: first published as 10.1136/thoraxjnl-2019-213771 on 18 October 2020. Downloaded from http://thorax.bmj.com/ on December 26, 2020 at University of Liverpool Library. Protected by copyright.

allergic inflammation is solely dependent on the downstream signalling autophagy and LC3B, these transgenic mice were crossbred. Intriguingly, the exacerbated inflammation caused by MTOR deficiency was also significantly ameliorated in *lc3b*$^{-/-}$ mice (figure 6A–6D), suggesting that MTOR exerts its effect on allergic inflammation, at least partly, through regulation of autophagy and LC3B.

The airway inflammation modulated by MTOR–autophagy depends on the production of IL25 in mice

There is extensive evidence that airway ECs initiate and perpetuate allergic inflammation through the production of proallergic cytokines, such as TSLP, IL25 and IL33.[17] We, therefore, examined those epithelial proallergic cytokines in the *mtor*$^{\triangle/\triangle}$ or *lc3b*$^{-/-}$ mice. As reported,[22] we found alveolar, rather than bronchial, ECs might be the major source of IL33 in the allergic mouse lungs (online supplementary figure S8A), indicating that IL33 was not the direct downstream molecule of MTOR–autophagy in mouse bronchial ECs. Besides, we found that the mRNA and protein levels of TSLP were neither affected by HDM exposure nor by deletion of *mtor* or *lc3b* (online supplementary figure S8B-S8E). However, IL25 was significantly induced on HDM challenge, and it was further increased or notably diminished in *mtor*$^{\triangle/\triangle}$(figure 7A) or *lc3b*$^{-/-}$ (figure 7B) mice, respectively, highly consistent with the levels of airway inflammation in these mice. In line with the in vivo findings, autophagy inhibitor spautin-1 markedly attenuated the expression of IL25 induced by IL13 or IL33 in HBE cells (figure 7C). Moreover, IL25 neutralisation antibody remarkably attenuated the exacerbated airway inflammation in the MTOR-deficiency mice on HDM challenge (figure 7D–7F), suggesting a critical role of this cytokine in mediating the allergic inflammation modulated by MTOR–autophagy.

DISCUSSION

Airway ECs represent the first barrier against environmental invaders, and autophagy can be induced in ECs by diverse stresses. Accumulating literature have demonstrated that autophagy is induced by various environmental stimuli in diverse pulmonary disorders, including in lung tissues of COPD patients,[23] and in mouse lungs or in cultured ECs exposed to cigarette smoking,[18 23–25] nanoparticles,[26] airborne particulate matter[27] and certain viruses.[28] Similar to these findings, our current study provides the first evidence that MTOR is inactivated in ECs from human asthmatics and allergic animals. Poon *et al* have observed increased AVs in ECs from asthmatics,[7] which agrees with our current findings. The induction of autophagy in asthma seems not principally by allergens, but most likely due to a synergistic effect of the allergic inflammation, as HDM exposure induced airway inflammation at 24 hours while autophagy was evidenced later at 48 hours. In fact, HDM even at very high concentrations failed to induce autophagy in HBE cells (data not shown), while IL13 and IL33 notably enhanced autophagy, further supporting this conclusion. Consequently, since HDM per se seems not to induce autophagy, our data also suggest that MTOR–autophagy in ECs may exert little effects on the initiation of allergic inflammation, but may solely orchestrate the later production of certain proallergic cytokines such as IL25, eventually modulating the further amplified inflammation.

The functions of autophagy in various lung disease pathogenesis are remaining either deleterious or cytoprotective, most likely depending on the different stimuli or cell type, as in asthma.[6] In a recent study, autophagy inhibitor 3-methyladenine has been shown to dose-dependently attenuate allergy-induced airway inflammation in mice.[29] Autophagy is required for IL13-mediated superoxide production via the NADPH oxidase DUOX1 in human tracheobronchial ECs.[30] Our current data further demonstrate that autophagy critically mediates the production of proallergic cytokines such as IL25, and subsequent further promotes the allergic inflammation, which is consistent with those studies in asthma research,[29 30] and is accordant with the deleterious role of autophagy in the pathogenesis of cigarette smoke-induced COPD,[18 19 23–25 31] nanoparticle-induced or environmental particulate-induced airway injury[26 27] and certain virus-induced lung infections.[28 32] However, the *lc3b*$^{-/-}$ mice display an enhanced AHR, regardless of the diminished airway inflammation, which may be due to the deficiency of this protein in other lung structure cells. To support this, *lc3b*$^{-/-}$ mice could promote the proliferation of lung fibroblast[33] and airway smooth muscle cells,[34] which theoretically may influence AHR in asthma pathogenesis. Autophagy inhibitor Spautin-1 also enhanced AHR, consistent with the results of *lc3b*$^{-/-}$ mice.

The roles of MTOR in asthma pathogenesis could also be cell type specific. Previous studies[10–13] have indicated that inhibition of MTOR with rapamycin attenuates allergic airway inflammation, while it was the first time our present study clearly demonstrates that airway-specific MTOR-deficiency promotes allergic airway inflammation in mice. One plausible explanation is that rapamycin inhibition of MTOR suppresses the inflammatory function of myeloid cells including eosinophils, while it causes elevated proallergic cytokine production in airway epithelium. To support this, pulmonary toxicity has been widely observed when rapamycin is used as an immunosuppressive drug for renal transplantation,[14] and research has shown that up to one-sixth of patients taking MTOR inhibitors get a reversible interstitial pneumonitis.[35] Thus, the present study both provides mechanistic explanations that MTOR inhibition could cause airway injury, and also reemphasises the awareness of possible severe adverse effects in increasing the sensitivity to allergies or other pulmonary pathogens in ongoing clinical trials of MTOR inhibitors or autophagy up-regulators.

It should be noted that IL25 is not solely produced by ECs. Though in cultured HBE cells, autophagy inhibitor can suppress IL13- and IL33-induced IL25 expression, this could not rule out the contributions of IL25 derived from resources other than epithelium in mediating the eventual allergic airway inflammation in vivo.

In summary, our present study demonstrates that certain allergic cytokines, such as early initiated IL33 and later produced IL13, suppresses MTOR and induces autophagy likely via TSC2 in airway ECs. The induction of autophagy results in the production of proallergic cytokines such as IL25 in the lung tissues, thereby promoting the type 2 response and eventually perpetuating airway inflammation in asthma (online supplementary figure S9). Activation of MTOR and/or inhibition of autophagy in ECs may therefore serve as a therapeutic strategy for asthmatic inflammation.

Author affiliations
[1]Key Laboratory of Respiratory Disease of Zhejiang Province, Department of Respiratory and Critical Care Medicine, Second Affiliated Hospital of Zhejiang University School of Medicine, Hangzhou, Zhejiang, China
[2]State Key Laboratory of Respiratory Disease, National Clinical Research Center for Respiratory Disease, Guangzhou, Guangdong, China
[3]Department of Respiratory Medicine, Weifang V E Hospital, Weifang, China
[4]Channing Laboratory, Brigham and Women's Hospital, Harvard Medical School, Boston, MA, USA
[5]Division of Pulmonary and Critical Care Medicine, Weill Cornell Medical College, New York, NY, USA

Thorax: first published as 10.1136/thoraxjnl-2019-213771 on 18 October 2020. Downloaded from http://thorax.bmj.com/ on December 26, 2020 at University of Liverpool Library. Protected by copyright.

Contributors ZC and HS designed and supervised the study; WL, YW, YZ, ZL, HC, HL, LD, MZ, YW, JZ, JX, YH and WH performed experiments; MQ, QZ, WH, BZ, JH, CW and MW assisted in collection of human samples; YW performed EM experiments; WL, YW, YZ and ZC prepared figures; WL, YW, YZ and ZC drafted manuscript; XZ, WQ, FY, SY, ZC, AMKC and HS analysed data and revised manuscript. All authors approved the final manuscript.

Funding This work was supported by the Major Project (81490532 to HS), the General Projects (31970826 to ZC, 81370126 to WL and 81570021 to HH) and the Key Project (81930003 to HS) from the National Natural Science Foundation of China, and the National Key Research and Development Plan of China (2016YFC0905800 and 2016YFA0501602).

Competing interests AMKC is a cofounder, stock holder and serves on the Scientific Advisory Board for Proterris, which develops therapeutic uses for carbon monoxide. AMKC also has a use patent on CO. No other authors have any conflicts of interests.

Patient consent for publication Not required.

Ethics approval All experimental protocols were approved by the Ethical Committee for Animal Studies at Zhejiang University.

Provenance and peer review Not commissioned; externally peer reviewed.

Data availability statement All data relevant to the study are included in the article or uploaded as supplementary information.

ORCID iD
Zhouyang Li http://orcid.org/0000-0002-7721-0175

REFERENCES

1 Barnes PJ. Immunology of asthma and chronic obstructive pulmonary disease. *Nat Rev Immunol* 2008;8:183–92.
2 Lambrecht BN, Hammad H. The airway epithelium in asthma. *Nat Med* 2012;18:684–92.
3 Lambrecht BN, Hammad H. The immunology of asthma. *Nat Immunol* 2015;16:45–56.
4 Saxton RA, Sabatini DM. mTOR signaling in growth, metabolism, and disease. *Cell* 2017;168:960–76.
5 Choi AMK, Ryter SW, Levine B. Autophagy in human health and disease. *N Engl J Med* 2013;368:651–62.
6 Racanelli AC, Kikkers SA, Choi AMK, *et al*. Autophagy and inflammation in chronic respiratory disease. *Autophagy* 2018;14:221–32.
7 Poon AH, Chouiali F, Tse SM, *et al*. Genetic and histologic evidence for autophagy in asthma pathogenesis. *J Allergy Clin Immunol* 2012;129:569–71.
8 Dickinson JD, Alevy Y, Malvin NP, *et al*. Il13 activates autophagy to regulate secretion in airway epithelial cells. *Autophagy* 2016;12:397–409.
9 Suzuki Y, Maazi H, Sankaranarayanan I, *et al*. Lack of autophagy induces steroid-resistant airway inflammation. *J Allergy Clin Immunol* 2016;137:1382–9.
10 Fujitani Y, Trifilieff A. In vivo and in vitro effects of SAR 943, a rapamycin analogue, on airway inflammation and remodeling. *Am J Respir Crit Care Med* 2003;167:193–8.
11 Mushaben EM, Kramer EL, Brandt EB, *et al*. Rapamycin attenuates airway hyperreactivity, goblet cells, and IgE in experimental allergic asthma. *J Immunol* 2011;187:5756–63.
12 Yamaki K, Yoshino S. Preventive and therapeutic effects of rapamycin, a mammalian target of rapamycin inhibitor, on food allergy in mice. *Allergy* 2012;67:1259–70.
13 Hua W, Liu H, Xia L-X, *et al*. Rapamycin inhibition of eosinophil differentiation attenuates allergic airway inflammation in mice. *Respirology* 2015;20:1055–65.
14 Pham P-TT, Pham P-CT, Danovitch GM, *et al*. Sirolimus-associated pulmonary toxicity. *Transplantation* 2004;77:1215–20.
15 Kilkenny C, Browne WJ, Cuthill IC, *et al*. Improving bioscience research reporting: the ARRIVE guidelines for reporting animal research. *PLoS Biol* 2010;8:e1000412.
16 Klionsky DJ, Abdelmohsen K, Abe A, *et al*. Guidelines for the use and interpretation of assays for monitoring autophagy (3rd edition). *Autophagy* 2016;12:1–222.
17 Lambrecht BN, Hammad H, Fahy JV. The cytokines of asthma. *Immunity* 2019;50:975–91.
18 Chen Z-H, Lam HC, Jin Y, *et al*. Autophagy protein microtubule-associated protein 1 light chain-3B (LC3B) activates extrinsic apoptosis during cigarette smoke-induced emphysema. *Proc Natl Acad Sci U S A* 2010;107:18880–5.
19 Lam HC, Cloonan SM, Bhashyam AR, *et al*. Histone deacetylase 6-mediated selective autophagy regulates COPD-associated cilia dysfunction. *J Clin Invest* 2013;123:5212–30.
20 Liu J, Xia H, Kim M, *et al*. Beclin1 controls the levels of p53 by regulating the deubiquitination activity of USP10 and USP13. *Cell* 2011;147:223–34.
21 Xu X-C, Wu Y-F, Zhou J-S, *et al*. Autophagy inhibitors suppress environmental particulate matter-induced airway inflammation. *Toxicol Lett* 2017;280:206–12.
22 Cayrol C, Girard J-P. Interleukin-33 (IL-33): a nuclear cytokine from the IL-1 family. *Immunol Rev* 2018;281:154–68.
23 Chen Z-H, Kim HP, Sciurba FC, *et al*. Egr-1 regulates autophagy in cigarette smoke-induced chronic obstructive pulmonary disease. *PLoS One* 2008;3:e3316.
24 Mizumura K, Cloonan SM, Nakahira K, *et al*. Mitophagy-dependent necroptosis contributes to the pathogenesis of COPD. *J Clin Invest* 2014;124:3987–4003.
25 Kim HP, Wang X, Chen Z-H, *et al*. Autophagic proteins regulate cigarette smoke-induced apoptosis: protective role of heme oxygenase-1. *Autophagy* 2008;4:887–95.
26 Li C, Liu H, Sun Y, *et al*. Pamam nanoparticles promote acute lung injury by inducing autophagic cell death through the Akt-TSC2-mTOR signaling pathway. *J Mol Cell Biol* 2009;1:37–45.
27 Chen Z-H, Wu Y-F, Wang P-L, *et al*. Autophagy is essential for ultrafine particle-induced inflammation and mucus hyperproduction in airway epithelium. *Autophagy* 2016;12:297–311.
28 Sun Y, Li C, Shu Y, *et al*. Inhibition of autophagy ameliorates acute lung injury caused by avian influenza A H5N1 infection. *Sci Signal* 2012;5:ra16.
29 Jiang X, Fang L, Wu H, *et al*. Tlr2 regulates allergic airway inflammation and autophagy through PI3K/Akt signaling pathway. *Inflammation* 2017;40:1382–92.
30 Dickinson JD, Sweeter JM, Warren KJ, *et al*. Autophagy regulates DUOX1 localization and superoxide production in airway epithelial cells during chronic IL-13 stimulation. *Redox Biol* 2018;14:272–84.
31 Zhou J-S, Zhao Y, Zhou H-B, *et al*. Autophagy plays an essential role in cigarette smoke-induced expression of MUC5AC in airway epithelium. *Am J Physiol Lung Cell Mol Physiol* 2016;310:L1042–52.
32 Ma J, Sun Q, Mi R, *et al*. Avian influenza A virus H5N1 causes autophagy-mediated cell death through suppression of mTOR signaling. *J Genet Genomics* 2011;38:533–7.
33 Patel AS, Lin L, Geyer A, *et al*. Autophagy in idiopathic pulmonary fibrosis. *PLoS One* 2012;7:e41394.
34 Lee S-J, Smith A, Guo L, *et al*. Autophagic protein LC3B confers resistance against hypoxia-induced pulmonary hypertension. *Am J Respir Crit Care Med* 2011;183:649–58.
35 Barber NA, Ganti AK. Pulmonary toxicities from targeted therapies: a review. *Target Oncol* 2011;6:235–43.

Thorax: first published as 10.1136/thoraxjnl-2019-213771 on 18 October 2020. Downloaded from http://thorax.bmj.com/ on December 26, 2020 at University of Liverpool Library. Protected by copyright.

BMJ Publishing Group Limited (BMJ) disclaims all liability and responsibility arising from any reliance placed on this supplemental material which has been supplied by the author(s)

Online Data Supplement

MTOR suppresses autophagy-mediated airway epithelial injury in allergic inflammation

Wen Li[1, #], Yin-Fang Wu[1, #], Yun Zhao[1, #], Zhou-Yang Li[1], Hai-Xia Chen[1], Ling-Ling Dong[1], Hui-Wen Liu[1], Min Zhang[1], Yan-Ping Wu[1], Jie-Sen Zhou[1], Juan Xiong[1], Yue Hu[1], Wen Hua[1] , Bin Zhang[1] , Min-Zhi Qiu[2] , Qing-Ling Zhang[2] , Chun-Hua Wei[3] , Ming-Chun Wen[3] , Jing Han[3] , Xiao-Bo Zhou[4] , Wei-Liang Qiu[4], Fu-Gui Yan[1] , Hua-Qiong Huang[1] , Song-Min Ying[1] , Augustine M. K. Choi[5,*] , Hua-Hao Shen[1, 2,*] , Zhi-Hua Chen[1,*]

[1] Key Laboratory of Respiratory Disease of Zhejiang Province, Department of Respiratory and Critical Care Medicine, Second Affiliated Hospital of Zhejiang University School of Medicine. [2]State Key Lab of Respiratory Disease, National Clinical Research Center for Respiratory Disease, Guangzhou, China. [3]Department of Respiratory Medicine, Weifang V E Hospital, Weifang, China. [4]Channing Laboratory, Brigham and Women's Hospital, Harvard Medical School, Boston, USA. [5]Joan and Sanford I. Weill Department of Medicine, New York-Presbyterian Hospital, Weill Cornell Medical College, New York, USA.

Authorship note: [#]These authors contributed equally to this article.

*Corresponding authors:

Zhi-Hua Chen, Email: zhihuachen@zju.edu.cn; Hua-Hao Shen, Email:

BMJ Publishing Group Limited (BMJ) disclaims all liability and responsibility arising from any reliance placed on this supplemental material which has been supplied by the author(s)

huahaoshen@zju.edu.cn; Augustine M. K. Choi, Email: amc2056@med.cornell.edu

Zhi-Hua Chen, PhD, Department of Respiratory and Critical Care Medicine, Key Laboratory of Respiratory Disease of Zhejiang Province, Second Affiliated Hospital, Zhejiang University School of Medicine, 88 Jiefang Rd., Hangzhou 310009, China. Tel.: 86-571-8898-1913; Fax: 86-571-8778-3729

BMJ Publishing Group Limited (BMJ) disclaims all liability and responsibility arising from any reliance placed on this supplemental material which has been supplied by the author(s)

Supplemental material and methods

Reagents

Antibodies used were as follows: ACTB (Santa Cruz Biotechnology, sc-47778), p-S6 (Cell Signaling Technology, 4858), MTOR (Cell Signaling Technology, 2983), p-MTOR (Cell Signaling Technology, 5536), LC3B (Sigma-Aldrich, L7543), CC10 (Santa Cruz Biotechnology, sc-365992), TSC2 (Cell Signaling Technology, 3990), p-TSC2 (Cell Signaling Technology, 3611), p-TSC2 (Abcam, ab109403), IL25 neutralization antibody (R&D systems, MAB13992), Rat isotype control (R&D systems, MAB0061). RNAiso plus (9109), Reverse Transcription Reagents (DRR037A), and SYBR Green Master Mix (DRR041A) were purchased from Takara Biotechnology. Primers for *Tslp, Il13, Il25, Il33,* and *Muc5ac* were synthesized by Sangon Biotech, Shanghai. ELISA kits for mouse TSLP (MTLP00), IL13 (DY413), IL25 (DY1399), and mouse IL33 (M3300) were purchased from R&D systems. Doxycycline (D9891) and Baf A1 (B1793) were purchased from Sigma-Aldrich. Spautin1 (S7888) was purchased from Selleck. Recombinant Human IL33 (C091), human IL4 (CX03), and human TNF-α (C036) was purchased from Novoprotein, and recombinant Human IL13 (200-13) was a product from Peprotech.

Human samples

The diagnosis of bronchial asthma was based on the Global Initiative for Asthma (GINA) guidelines. The patients were relatively severe asthma who received a

BMJ Publishing Group Limited (BMJ) disclaims all liability and responsibility arising from any reliance placed on this supplemental material which has been supplied by the author(s)

bronchoscope to further confirm the clinical diagnosis. Exclusion criteria included systemic inflammation or other respiratory diseases. Healthy control subjects were participants with benign pulmonary nodules, who had normal lung function and no respiratory symptoms. We collected 3 sets of paraffin-embedded slides of human airway samples from Weifang Asthma Hospital (Weifang, China), State Key Lab of Respiratory Disease (Guangzhou, China), and the Second Affiliated Hospital of Zhejiang University (Hangzhou, China). We used the 1st set of samples (3 controls and 12 asthmatics, each 2 slides) for staining of p-S6 and LC3B. However, the number of asthmatic samples of LC3B staining was 11, because there were no epithelial cells in 1 slide for LC3B staining. And we used the 2nd set of samples (7 controls and 15 asthmatics) for staining of p-TSC2. We also collected another set of fresh airway biopsies (4 healthy controls and 4 asthmatics) for electronic microscopy analysis. In all the 3 sets of human samples, both age and sex distributions were similar for asthmatic patients and controls. The study was approved by the ethics committee of the three institutions. Written informed consent was obtained from all asthmatic or control subjects. The clinical information of each set of human subjects was shown in Table 1-2 and S3.

Mice

mtor$^{flox/flox}$ mice (C57BL/6; The Jackson Laboratory) were crossed with CC10-rtTA/(tetO)$_7$-cre transgenic mice (C57BL/6) to generate CC10-rtTA/(tetO)$_7$-cre-*mtor*$^{flox/flox}$ (*mtor*$^{\Delta/\Delta}$) mice. Transgene-negative littermates were used as the control (*mtor*$^{+/+}$) animals in the experiments. To induce expression of Cre,

BMJ Publishing Group Limited (BMJ) disclaims all liability and responsibility arising from any reliance placed on this supplemental material which has been supplied by the author(s)

6-wk-old *mtor*$^{\Delta/\Delta}$ mice and age- and sex-matched *mtor*$^{+/+}$ mice were fed with doxycycline in drinking water (2 mg/ml) for 20 days in advance of establishing the model of asthma, and the mice were maintained on doxycycline at all the time until they were killed. *lc3b*$^{-/-}$ mice were from Jackson laboratory. C57BL/6 mice were used as WT mice, which were purchased from Shanghai SLAC laboratory animal Co. Ltd. To delete both of the *mtor* and *lc3b* alleles in airway epithelial cells, CC10-rtTA/(tetO)7-cre-*mtor*$^{flox/flox}$- *lc3b*$^{-/-}$ (*mtor*$^{\Delta/\Delta}$*lc3b*$^{-/-}$) mice were generated by crossing the *mtor*$^{\Delta/\Delta}$ mice with *lc3b*$^{-/-}$ mice. CD45.1 mice were kindly provided by Dr. Lie Wang, Zhejiang University. All mice used in this study were 6-8-wk-old male and were housed under a constant 12-hour light/12-hour dark cycle in a specific pathogen-free facility and all experimental protocols were approved by the Ethical Committee for Animal Studies at Zhejiang University. During the process of animal studies no adverse events occurred.

Transmission electron microscopy

For transmission electron microscopy (TEM) examination, the freshly isolated bronchus samples from mouse and fiberoptic bronchial biopsy specimens of asthmatic patients and healthy control were fixed in 2.5% glutaraldehyde in PBS overnight and embedded in paraffin. These samples were photographed using a TECNA1 10 transmission electron microscope (FEI, Hillsboro, Oregon, USA). For quantification, the area of the cell cytoplasm of ciliated cells was measured using Image-Pro Plus 6.0 (Media Cybernetics, Silver Spring, MD, USA), and all autophagic vacuoles (AVs) in human ciliated cells were counted. Data were represented as AVs

BMJ Publishing Group Limited (BMJ) disclaims all liability and responsibility arising from any reliance placed on this supplemental material which has been supplied by the author(s)

per 100 μm^2. While in mouse ciliated cells, Autophagosomes (APs) and autolysosomes (ALs) were counted. [1-3] The data were represented as APs and ALs per 100 μm^2, respectively.

Cell culture

HBE cells were purchased from American Type Culture Collection (ATCC@ PCS-300-100™) and were cultured in RPMI 1640 with 10% FBS. Each well of six-well plates was placed with 5×10^5 cells for 18h and treated with IL13 (10 ng/ml) or IL33 (100 ng/ml).

GFP-LC3 plasmid transfection

The GFP-LC3B plasmid transfection was performed with the PolyJet in vitro DNA Transfection reagent following the manufacturer's protocol. Briefly, cells were seeded to each well of six-well plates for 24 h before transfection. The infection medium was replaced with fresh growth medium after being incubated with HBE cells for 8 h. Confocal images were viewed using a Zeiss LSM confocal laser scanning microscope (Carl Zeiss, Göttingen, Germany).

Allergic animal models

Mice for HDM model were exposed to HDM (Greer Laboratories, 10.52 EU/mg endotoxin) via intratracheal injection of HDM (100 μg) in 50 μl saline (control mice injected pure saline) on days 0, 7 and 14 and were sacrificed on day 17 as previously described.[4] Mice for OVA model were sensitized on day 0 and day 14 by

BMJ Publishing Group Limited (BMJ) disclaims all liability and responsibility arising from any reliance placed on this supplemental material which has been supplied by the author(s)

intraperitoneal injection of 80 μg OVA in 0.1 ml saline and equal volume of aluminum hydroxide. On days 24, 25, and 26, mice were nebulized with 1.5% OVA in saline for 45 min. Control mice were sensitized and challenged with saline instead of OVA. Mice were analyzed in 24h after the last challenge.[5]

Measurement of airway hyperresponsiveness

we examined the airway hyperresponsiveness (AHR) by invasive plethysmography 48 h after the final HDM challenge using the Buxco FinePoint (Buxco Electronics, Troy, NY) as described previously.[6]

Bone marrow transplantation

Bone marrow transplantation (BMT) was performed by transplanting total BMCs (5×10^6) from 6-week-old mice (donor) into lethally irradiated (X-ray radiation at the dose of 8 Gy) 6-week-old mice (recipient) through tail vein. Allergic models were established by three weeks after BMT. Transplantation efficiency was evaluated by detecting the ratio of reconstituted $CD45.1^+$ or $CD45.2^+$ / total $CD45^+$ cells in bone marrow when mice were sacrificed.

In vivo spautin-1 treatment

Spautin-1 was dissolved in DMSO and was injected intraperitoneally (20 mg/kg) on days 12, 13, and 14 before the last HDM challenge. The controls were received the same volume of DMSO.

In vivo IL25 neutralization antibody treatment

BMJ Publishing Group Limited (BMJ) disclaims all liability and responsibility arising from any reliance placed on this supplemental material which has been supplied by the author(s)

IL25 neutralization antibody (2 μg) was dissolved in 50 μl PBS and was injected intratracheally on day 13, 14, 15, and 16. The controls were received the same volume of normal Rat isotype control or Goat isotype control, respectively.

BALF collection and analysis

72 h after the last exposure to HDM or 24 h after the last OVA challenge, mice were sacrificed to obtain BALF by injecting 0.4 ml PBS into the left lungs and withdrawing to collect the cells for three times. After counting the number of BALF total cells, the residual BALF was centrifuged at 6000 rpm for 10 min at 4℃. The supernatant was stored at -80℃ for the detection of LDH and cell precipitation suspended in PBS was spun onto glass slides. Cells were stained with Wright-Giemsa stain (Baso, BA4017) for differential counts by counting total of 200 cells.

Histological analyses

After treatment with HDM or OVA, the left lungs of experimental mice were fixed in formalin for 24 h, embedded in paraffin, and then stained with H&E or PAS according to standard procedures. The degree of peribronchial and perivascular inflammation was assessed on a subjective scale of 0–3 as previously described.[7] PAS-stained goblet cells in airway epithelium were measured using a numerical scoring system (0 =＜5% goblet cells; 1 = 5–25%; 2 = 25–50%; 3 = 50–75%; 4 =＞75%＝, as described previously.[8] All quantification of histology was measured by observers blinded to group/treatment.

RNA isolation and quantitative real-time PCR analysis

BMJ Publishing Group Limited (BMJ) disclaims all liability and responsibility arising from any reliance placed on this supplemental material which has been supplied by the author(s)

Total RNA was extracted from lung homogenates by RNAiso plus. RNA was reverse-transcribed with Reverse Transcription Reagents and cDNA was used for quantitative real-time PCR with SYBR Green Master Mix on a StepOne Real-Time PCR System (Applied Biosystems, Foster City, CA) to determine the levels of mouse *Il13*, *Il33*, *Il25*, *Tslp*, and *Muc5ac.* All procedures were according to the manufacturer's protocols. Data were normalized to *Actb* expression. The primers are listed in Table S1.

Immunohistochemistry (IHC) staining

Lung tissues and fiberoptic bronchial biopsy specimens of asthmatic patients and healthy controls were fixed in 4% paraformaldehyde and embedded in paraffin. Then lung sections were immunostained with antibodies against p-S6, LC3B, and p-TSC2 using the standard methods.[9] These samples imaged using an Olympus BX53 inverted microscope (Olympus, Melville, NY). Image quantitative analysis was performed by observers blinded to group/treatment. To evaluate the alteration of the expression of p-S6, LC3B, and p-TSC2, results were provided as the percentage of positive cells in total epithelial cells.

Immunofluorescence staining

Lung sections were stained together with anti-p-S6 and anti-CC10 according to the manufacturer's protocol. Fluorescent images were captured with a Zeiss LSM laser scanning confocal microscope.

Western blot assay

BMJ Publishing Group Limited (BMJ) disclaims all liability and responsibility arising from any reliance placed on this supplemental material which has been supplied by the author(s)

Lung tissue homogenates were prepared with RIPA lysis buffer (Beyotime, P0013B) in the presence of protease-inhibitor cocktail (Roche Diagnostics GmbH, 04-693-116-001). Lysates were loaded to SDS–PAGE and immunoblotted with relevant antibodies using standard methods.

ELISA

Lung tissue homogenates were prepared by adding 300 μl RIPA to every 10 mg lung tissues. The concentration of TSLP, IL25, IL33, and IL13 in lung homogenates was determined with ELISA kits following the manufacturer's protocol.

Supplemental references

1. Chen ZH, Lam HC, Jin Y, et al. Autophagy protein microtubule-associated protein 1 light chain-3B (LC3B) activates extrinsic apoptosis during cigarette smoke-induced emphysema. *Proc Natl Acad Sci U.S.A* 2010;107:18880-18885.
2. Lam HC, Cloonan SM, Bhashyam AR, et al. Histone deacetylase 6-mediated selective autophagy regulates COPD-associated cilia dysfunction. *J Clin Invest* 2013;123:5212-5230.
3. Sun Y, Li C, Shu Y, et al. Inhibition of autophagy ameliorates acute lung injury caused by avian influenza A H5N1 infection. *Sci Signal* 2012;5:ra16.
4. Hammad H, Chieppa M, Perros F, et al. House dust mite allergen induces asthma via Toll-like receptor 4 triggering of airway structural cells. *Nat Med* 2009;15:410-416.
5. Lee JJ, Dimina D, Macias MP, et al. Defining a link with asthma in mice

BMJ Publishing Group Limited (BMJ) disclaims all liability and responsibility arising from any reliance placed on this supplemental material which has been supplied by the author(s)

congenitally deficient in eosinophils. *Science* 2004;305:1773-1776.

6. Tian BP, Xia LX, Bao ZQ, et al. Bcl-2 inhibitors reduce steroid-insensitive airway inflammation. *J Allergy Clin Immunol* 2017;140:418-430.

7. Lee KS, Lee HK, Hayflick JS, et al. Inhibition of phosphoinositide 3-kinase delta attenuates allergic airway inflammation and hyperresponsiveness in murine asthma model. *FASEB J* 2006; 20:455-465.

8. McMillan SJ, Bishop B, Townsend MJ, et al. The absence of interleukin 9 does not affect the development of allergen-induced pulmonary inflammation nor airway hyperreactivity. *J Exp Med* 2002;195:51-57.

9. Hu Y, Lou J, Mao YY, et al. Activation of MTOR in pulmonary epithelium promotes LPS-induced acute lung injury. *Autophagy* 2016;12(12):2286-2299.

Supplementary figures

Figure S1. Semi-quantification. (A) Semi-quantification of figure 3D. (B) Semi-quantification of figure 3H. Error bars, median ± IQR.

Figure S2. Inflammatory cytokines IL4 and TNF-α are not able to inactivate MTOR and induce autophagy in HBE cells. (A and B) Immunoblotting analysis of MTOR-autophagy-related molecules in HBE cells treated with IL4 (A) or TNF-α (B) at 100 ng/ml for indicated time points.

Figure S3. Activation of TSC2 in the airway epithelium of asthmatic patients or allergic mice, or in HBE cells treated with IL13. (A and B) Representative images (A) and semi-quantification (B) of the expression of immunohistochemistry staining of

BMJ Publishing Group Limited (BMJ) disclaims all liability and responsibility arising from any reliance placed on this supplemental material which has been supplied by the author(s)

p-TSC2 in bronchial specimens from asthmatic patients. Scale bar: 50 μm. Data are representative of 7 healthy controls and 15 asthmatic patients. (C and D) Representative images (C) and semi-quantification (D) of the expression of immunohistochemistry staining of p-TSC2 in mouse lung sections 72 h after HDM challenge. Scale bar: 50 μm. Data are representative of 6 mice per group. (E-G) Western blot analyses of the levels of TSC2 and p-TSC2 in IL13-treated HBE cells (E), and the semi-quantification results (F and G). Data are representative of 3-4 independent experiments. Error bars, mean ± SEM (B and D) or median ± IQR (F).

Figure S4. The generation of airway epithelium-specific *mtor*$^{\triangle/\triangle}$ mice. (A) Schematic map of the generation of *mtor*$^{\triangle/\triangle}$ mice. (B) Genotyping of *mtor*$^{\triangle/\triangle}$ mice by PCR using genomic DNA from mouse tails. (C) Representative immunofluorescence images of p-S6 (red), nuclei (DAPI, blue), airway epithelial cells (with clara cell antigen 10, CC10, green) in *mtor*-deficient airway epithelium. Data are representative of 3 independent experiments.

Figure S5. Expression of certain cytokines and airway responsive in HDM-exposed *mtor*$^{\triangle/\triangle}$or *lc3b*$^{-/-}$ mice. (A-C) Relative mRNA expression of *Il13* (A), *Il33* (B), or *Muc5ac* (C) in *mtor*$^{\triangle/\triangle}$ mouse lungs. (D-H) Relative mRNA expression of *Il13* (D) *Il33* (E), *Muc5ac* (F), *Eotaxin 1* (G), or *Il5* (H) in *lc3b*$^{-/-}$ mouse lungs. Data are representative of 4-12 mice and were replicated in 3 independent experiments. Error bars, mean ± SEM (A to D, J) or median ± IQR (E to I). *P < 0.05.

Figure S6. Spautin-1 attenuates HDM-induced airway inflammation.

BMJ Publishing Group Limited (BMJ) disclaims all liability and responsibility arising from any reliance placed on this supplemental material which has been supplied by the author(s)

HDM-induced allergic airway inflammation was described in Supplemental Methods. On days 12, 13, and 14, mice were intraperitoneally injected with spautin-1 (20 mg/kg) before the last HDM challenge. (A) The numbers of total cells and eosinophils in BALF. (B to E) Relative mRNA expression of *Il13* (B), *Il25* (C), *Il33* (D), and *Muc5ac* (E) in mouse lungs exposed to HDM. (F) AHR in response to methacholine in Spautin-1 treated mice was measured 48 h after the last exposure to HDM. Data are representative of 5-7 mice for each group and were replicated in 3 independent experiments. Error bars, mean ± SEM.

Figure S7. Bone marrow reconstitution of WT or *lc3b*$^{-/-}$ mice for allergic models. (A) Schematic image of the bone marrow transplantation (BMT). (B) Representative flow cytometry analysis of the expression of CD45.1 or CD45.2 in mouse bone marrow, and the efficiency of bone marrow transplantation (planted CD45.1^{+} or CD45.2^{+} / total CD45^{+} cells). Data were representative of 21 mice. (C) Amounts of eosinophils in BALF induced by HDM challenge. (D and E) Relative mRNA expression of *Il13* (D) and *Il25* (E) in mouse lungs exposed to HDM. Data are representative of 5-9 mice for each group and were replicated in 3 independent experiments. Error bars, median ± IQR.

Figure S8. Expression of IL33 and TSLP in *mtor*$^{\triangle/\triangle}$ and *lc3b*$^{-/-}$ mice. (A) Representative images of immunohistochemistry staining of IL33 in mouse lung sections 24 h after HDM challenge. Scale bar: 20 μm. (B and D) The mRNA expression of *Tslp* in mouse lung tissues of *mtor*$^{\triangle/\triangle}$ (B) and *lc3b*$^{-/-}$ (D) mice 72 h after

BMJ Publishing Group Limited (BMJ) disclaims all liability and responsibility arising from any reliance placed on this supplemental material which has been supplied by the author(s)

HDM challenge. (C and E) The protein expression of TSLP in BALF of *mtor*$^{\triangle/\triangle}$ (C) and *lc3b*$^{-/-}$ (E) mice 72 h after HDM challenge. Data are representative of 5-11 mice and were replicated in 3 independent experiments.

Figure S9. Summarization of the role of MTOR-LC3B axis in asthmatic epithelial injury. Allergen-initiated inflammatory mediators such as early initiated IL33 and later produced IL13 activate TSC2, which then suppresses MTOR and subsequently induces autophagy in airway epithelial cells. The induction of autophagy results in the production of certain pro-allergic cytokines such as IL25, thereby promoting the type 2 response and the overall airway inflammation in asthma

Table S1. Primers used for quantitative real-time PCR analysis.

Species	Genes	Primer sequence (5'-3')
Mouse	*Actb*	Forward AGAGGGAAATCGTGCGTGAC
		Reverse CAATAGTGATGACCTGGCCGT
Mouse	*Muc5ac*	Forward CTGTGACATTATCCCATAAGCCC
		Reverse AAGGGGTATAGCTGGCCTGA
Mouse	*Il13*	Forward CCTGGCTCTTGCTTGCCTT
		Reverse GGTCTTGTGTGATGTTGCTCA
Mouse	*Il33*	Forward ATTTCCCCGGCAAAGTTCAG
		Reverse AACGGAGTCTCATGCAGTAGA
Mouse	*Il25*	Forward TATGAGTTGGACAGGGACTTGA
		Reverse TGGTAAAGTGGGACGGAGTTG
Mouse	*Tslp*	Forward ACTGCAACTTCACGTCAATTACG

BMJ Publishing Group Limited (BMJ) disclaims all liability and responsibility arising from any reliance placed on this supplemental material which has been supplied by the author(s)

		Reverse TTGCTCGAACTTAGCCCCTTT
Human	*ACTB*	Forward CATGTACGTTGCTATCCAGGC
		Reverse CTCCTTAATGTCACGCACGAT
Human	*IL25*	Forward CCAGGTGGTTGCA-TTCTTGG
		Reverse TGGCTGTAGGTGTGGGTTCC

Table S2. Primers used for genotyping.

Genes	Primer sequence (5'-3')
Cc10	Forward AAA ATCTTGCCAGCTTTCCCC
	Reverse ACTGCCCATTGCCCAAACAC
Teto	Forward TGCCACGACCAAGTGACAGCAATG
	Reverse AGAGACGGA AATCCATCGCTCG
Mtor	Forward TTATGTTTGATAATTGCAGTTTTGGCTAGC AGT
	Reverse TTTAGGACTCCTTCTGTGACATAC ATTTCCT
Lc3b	Lc3b-1 GACACCTGTACACTCTGATGCACT
	Lc3b-2 CCTGCCGTCTGCTCTAAGCTG
	Lc3b-3 CCACTCCCACTGTCCTTTCCTAAT

Table S3. Characteristics of human subjects for p-TSC2 Expression.

	Healthy controls	Asthma	P-Value
Number	7	15	-
Age, yrs	52±3	49±2	0.547
Sex (M/F)	4/3	7/8	-

BMJ Publishing Group Limited (BMJ) disclaims all liability and responsibility arising from any reliance placed on this supplemental material which has been supplied by the author(s)

Bronchodilator reversibility test	negative	positive	-
Blood eosinophils (%)	1.77±0.62	7.23±1.72	0.048
FEV1, % predicted	86.38±7.38	65.74±5.22	0.034

Data are presented as Mean ± SEM. Differences between groups were assessed by t-test.

BMJ Publishing Group Limited (BMJ) disclaims all liability and responsibility arising from any reliance placed on this supplemental material which has been supplied by the author(s)

Figure S1

A

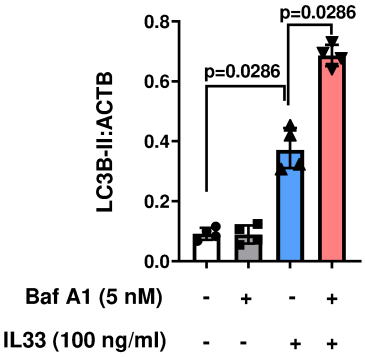

B

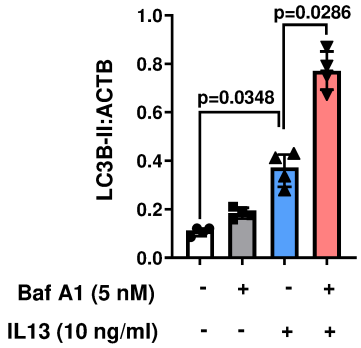

BMJ Publishing Group Limited (BMJ) disclaims all liability and responsibility arising from any reliance placed on this supplemental material which has been supplied by the author(s)

Figure S2

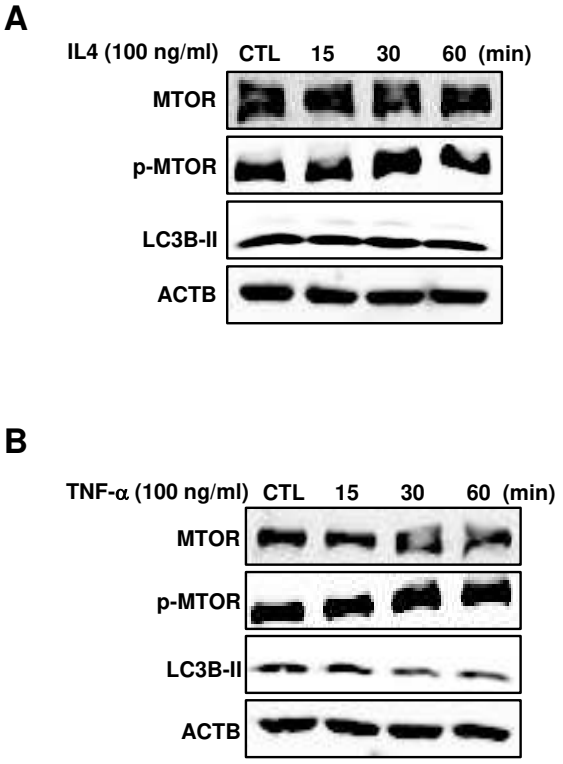

BMJ Publishing Group Limited (BMJ) disclaims all liability and responsibility arising from any reliance placed on this supplemental material which has been supplied by the author(s)

Figure S3

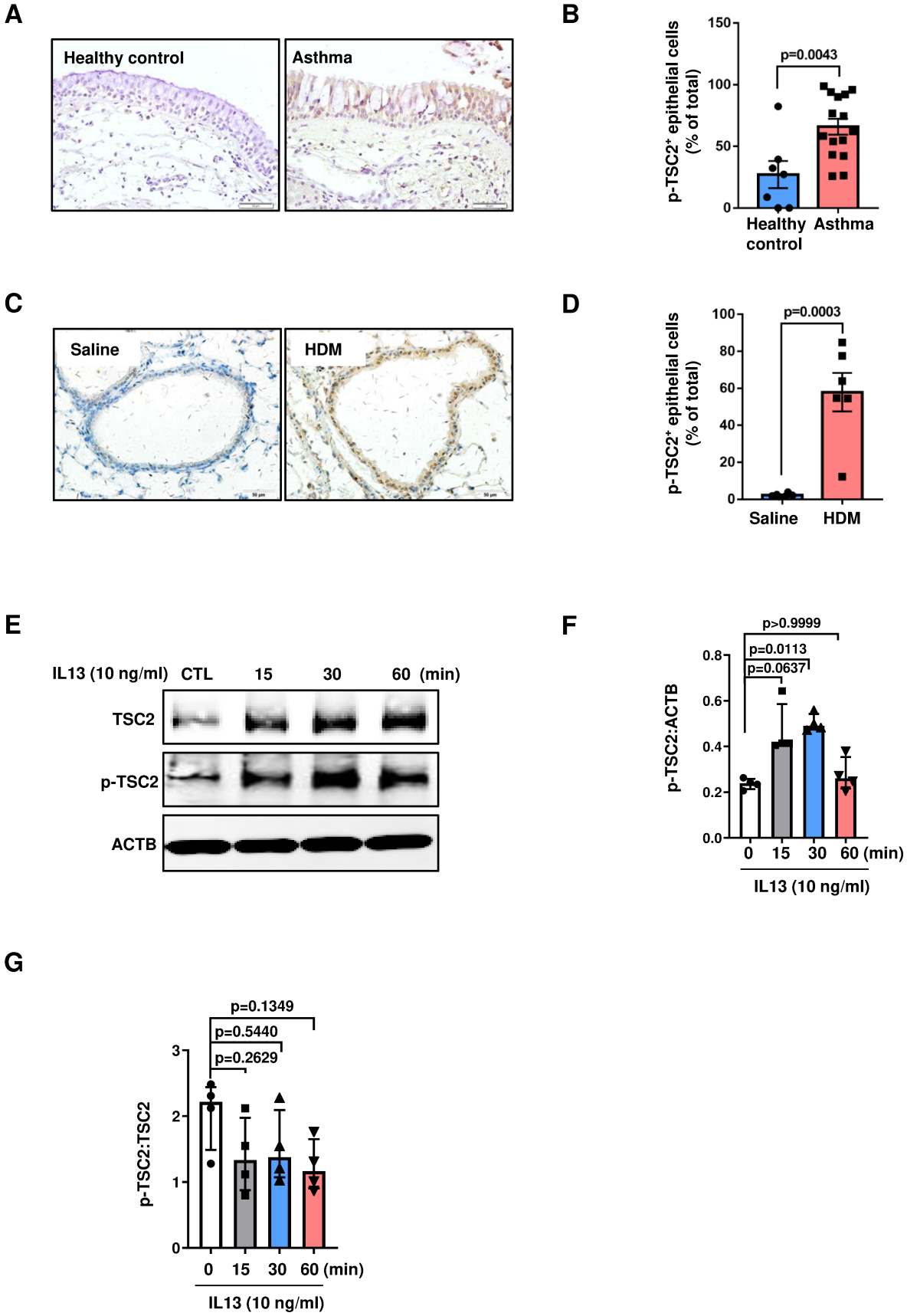

BMJ Publishing Group Limited (BMJ) disclaims all liability and responsibility arising from any reliance placed on this supplemental material which has been supplied by the author(s)

Figure S4

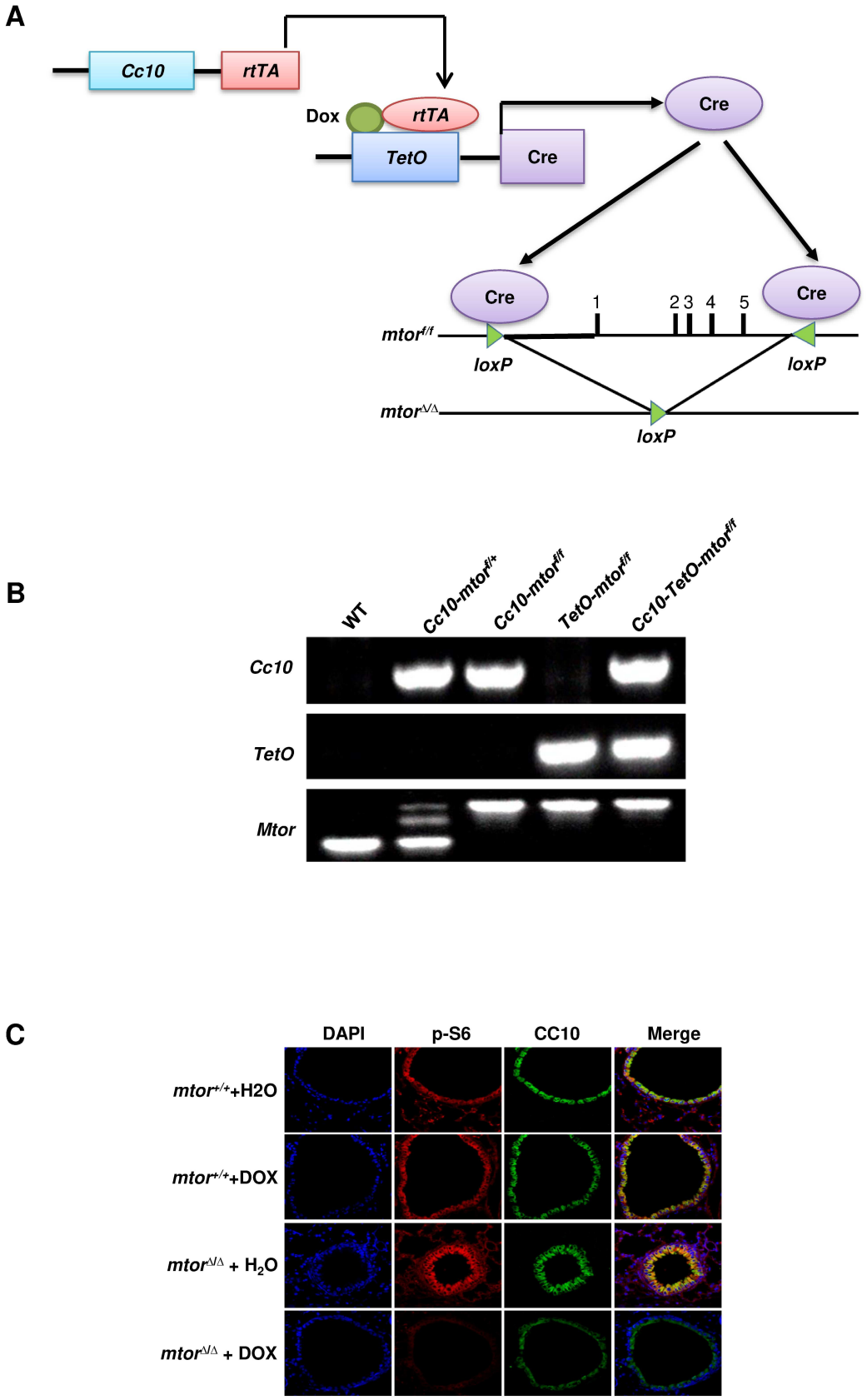

BMJ Publishing Group Limited (BMJ) disclaims all liability and responsibility arising from any reliance placed on this supplemental material which has been supplied by the author(s)

Figure S5

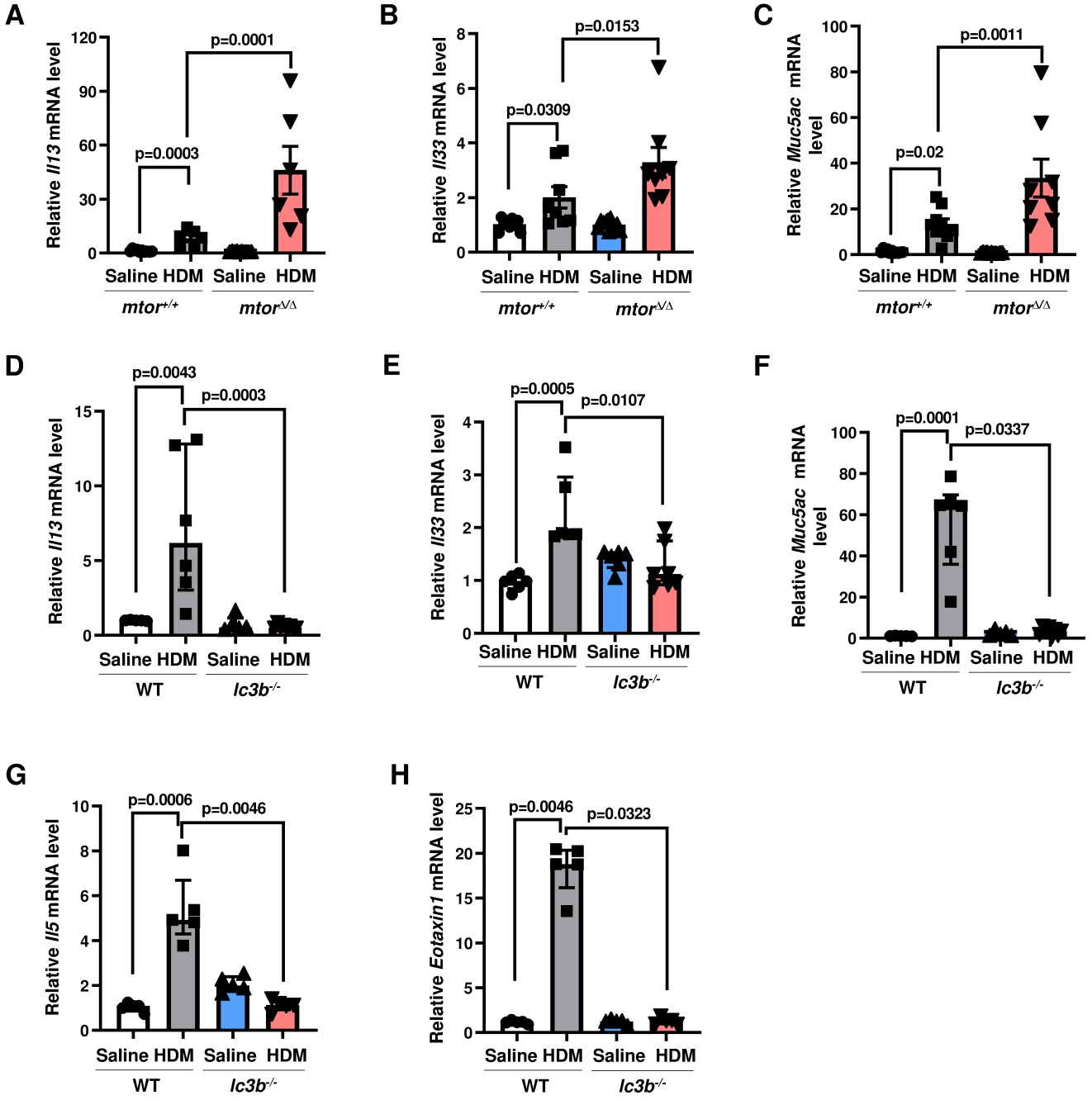

BMJ Publishing Group Limited (BMJ) disclaims all liability and responsibility arising from any reliance placed on this supplemental material which has been supplied by the author(s)

Figure S6

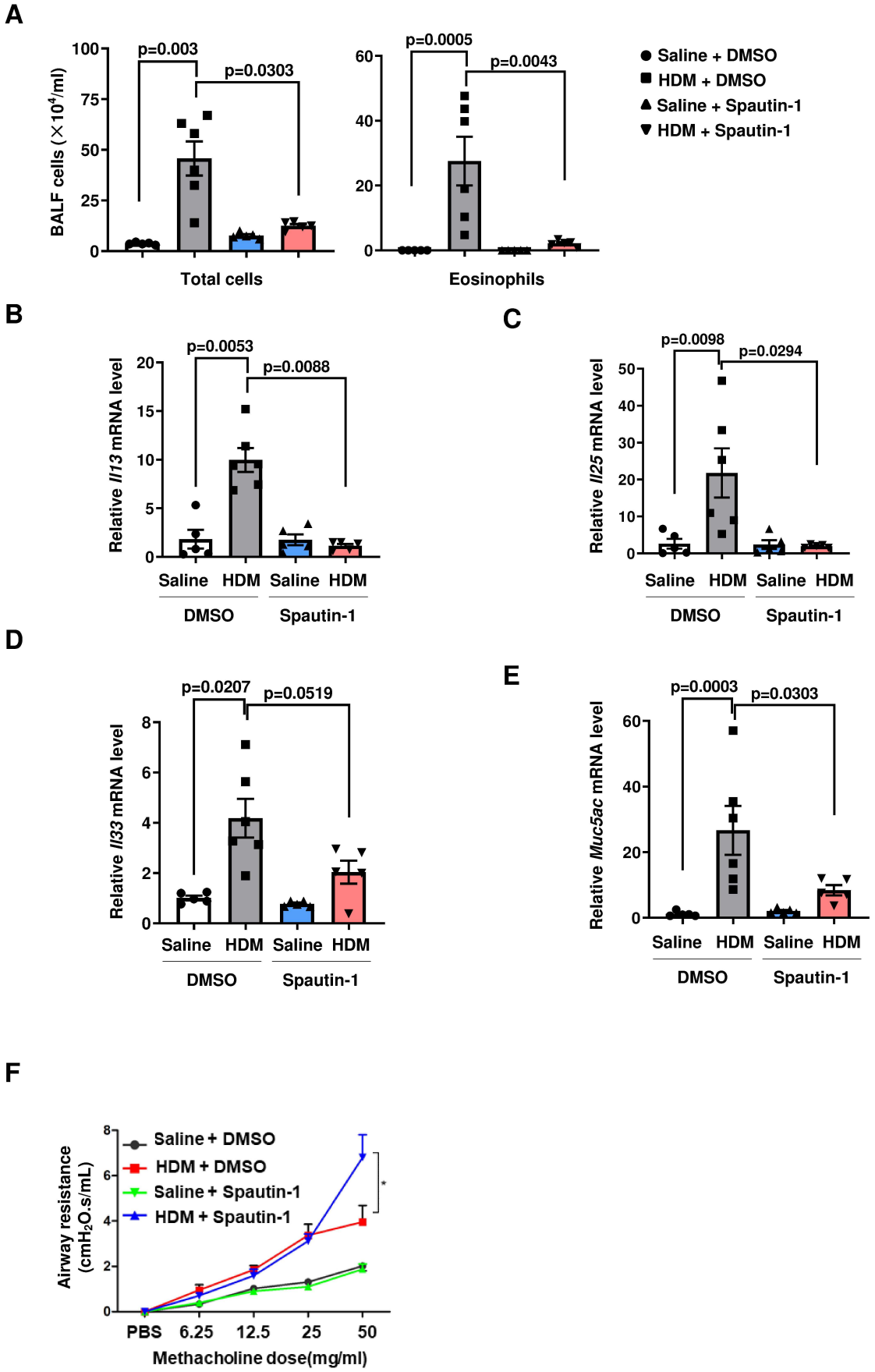

BMJ Publishing Group Limited (BMJ) disclaims all liability and responsibility arising from any reliance placed on this supplemental material which has been supplied by the author(s)

Figure S7

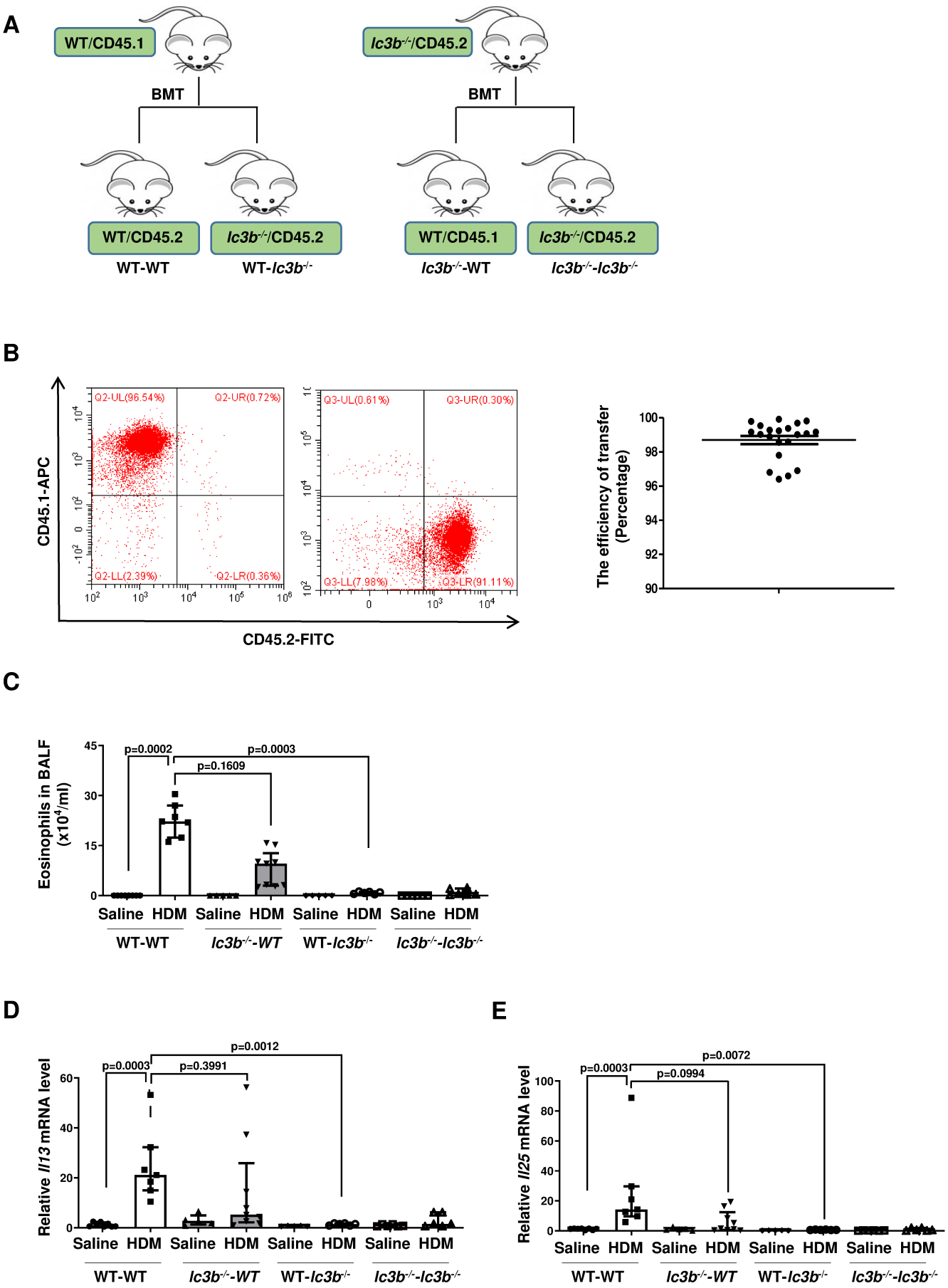

BMJ Publishing Group Limited (BMJ) disclaims all liability and responsibility arising from any reliance placed on this supplemental material which has been supplied by the author(s)

Figure S8

A

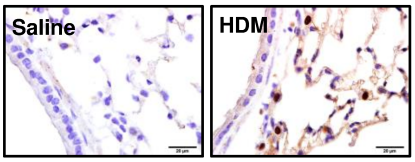

B

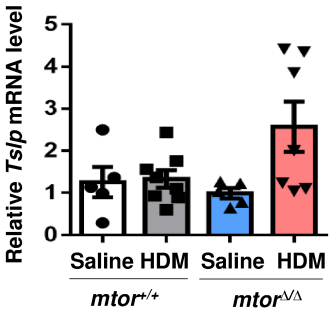

C

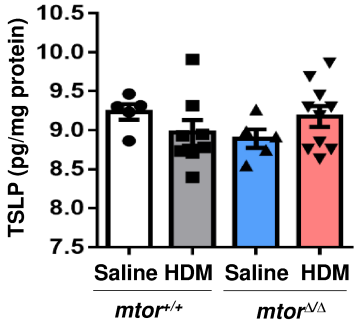

D

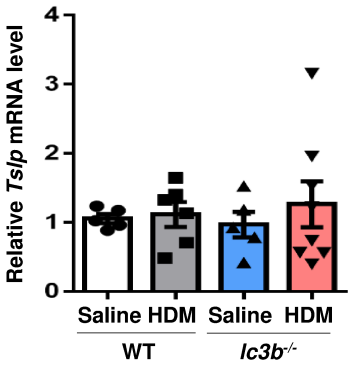

E

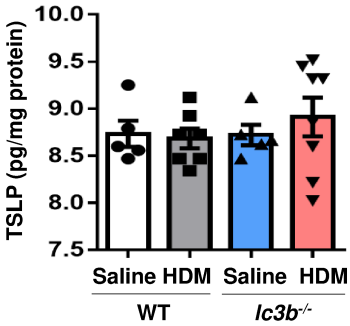

BMJ Publishing Group Limited (BMJ) disclaims all liability and responsibility arising from any reliance placed on this supplemental material which has been supplied by the author(s)
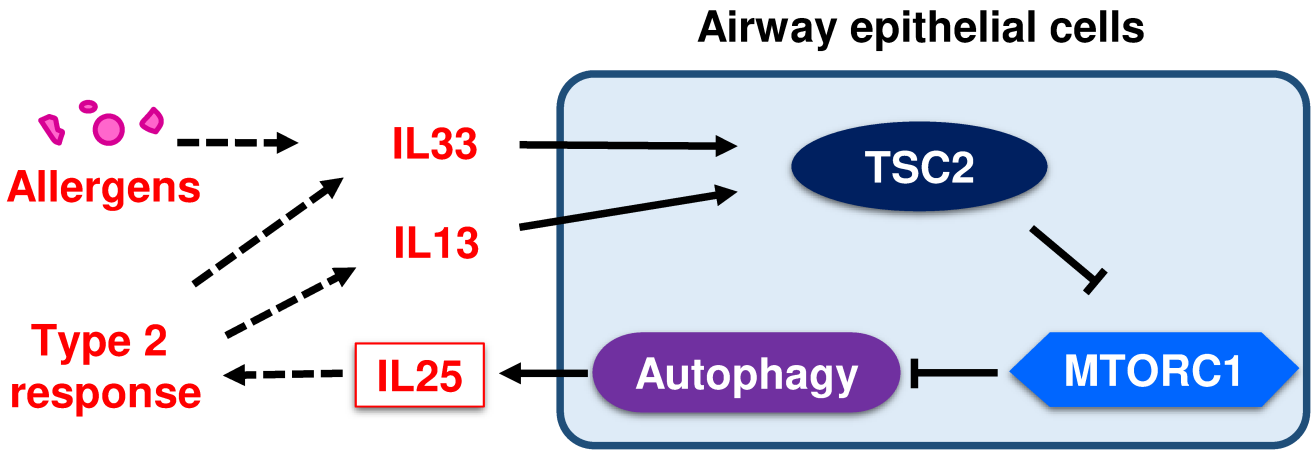
Figure S9